ORIGINAL PAPER

Petrophysical, seismic structural and facies analysis of the Miocene reservoirs of East Morgan oil field, Gulf of Suez, Egypt

Aref Adel Lashin · Ahmed Abd El-Naby

Abstract The Gulf of Suez is characterized by the presence of many hydrocarbon-bearing fields including reservoirs ranging in age from the Palaeozoic to the Tertiary. East Morgan oil field is one of the promising oil fields which are located in the southern part of the Gulf of Suez and tapping hydrocarbon deposits and potentials of the Miocene age. The purpose of this work is to evaluate the Miocene sediments of the Asl and Hawara Formations in East Morgan oil field (western sub-basin) through carrying out an integrated petrophysical, seismic structural and sequence stratigraphy study. Quantitative well logging analyses are carried out over Asl and Hawara Formations to throw light over their hydrocarbon potentiality. Good oil saturation is exhibited by the sand sections of Asl Formation, and fair to good are assigned for those of Hawara Formation in the Belayim dip province. On the other hand, a little hydrocarbon saturation is represented by both formations to the south of the study area in the Morgan accommodation zone (MAZ). The estimated petrophysical parameters of Asl reservoir throughout the study area range between 4 % and 10 % for effective porosity, 18 % and 89 % for shale volume and 2 % and 48 % for hydrocarbon saturation. Meanwhile, the ranges of 1–8 %, 20–98 % and 2–32 % are given for Hawara Formation for effective porosity, shale volume and

hydrocarbon saturation, respectively. The lateral distribution maps show that the central and the western parts of the MAZ attain the best petrophysical parameters and hydrocarbon potentiality. Seismic facies analysis, structural framework and depositional history of the study area were studied through interpreting the seismic reflection data of 27 seismic profiles. A number of geo-seismic cross sections are constructed and interpreted to investigate the structural setting of the study area and clarify the main structural elements that affect the hydrocarbon bearing reservoirs. A group of simple NW–SE step-like normal faults, parallel to the Clysmic trend, is found cutting through the reservoir rocks at the bottom layers of the section (Rudeis Formation) and extending upwards to overlying layers (Zeit Formation). Some graben- and horst-shaped structures are found and usually bounded by two sets of oppositely dipping normal step-like cross faults. The seismic facies and sequence analysis revealed that the Miocene rocks are subdivided into two major third-order depositional sequences (S1 and S2), separated by two major depositional sequence boundaries (DSB1 and DSB2). The first sequence (S1, Lower–Middle Miocene rocks) is of prime interest, as it encounters the main hydrocarbon reservoirs in the study area (Asl and Hawara Formations that are equivalent to Rudeis Formation). The seismic facies of this sequence are characterized by low to moderate amplitude, discontinuous horizons and bounded by the depositional sequence boundary (DSB1) at the top. The reflection geometry at the cycle boundaries is considered as erosional truncation, toplaps and even concordant along the upper boundary of the cycle. The external form of these sediments is considered as sheet-like and wedge-shaped units. The entrapment of hydrocarbons seems to be of a combined effect of the stratigraphic and structural elements. It appears clear that both of the step-like structural fault system and the lateral variation of facies are the key parameters that control the accumulation of hydrocarbon in this area and in East Morgan field as a whole.

A. A. Lashin (✉)
Geology Department, Faculty of Science, Benha University,
P.O. Box 13518, Benha, Qalubia, Egypt
e-mail: aref70@hotmail.com

A. A. Lashin
Geology and Geophysics Department, College of Science,
King Saud University, P.O. Box 2455, Riyadh 11451, Saudi Arabia

A. A. El-Naby
Geology Department, Faculty of Science, Ain Shams University,
Abbassia sq. 11566, Cairo, Egypt

Introduction

The Gulf of Suez rift is a Neogene continental rift that is developed by separation of the African Plate and the Sinai sub-Plate in the Late Oligocene–Early Miocene. It represents a northwest-elongated structural depression at the northern end of the Red Sea that is 350 km long and ranges in width from 52 km in the north to 90 km in the south. Opening of the Suez rift was initiated in response to N60°E extension before Early Miocene times (Robson 1971; Moustafa 1976; Garfunkel and Bartov 1977; Lyberis 1988; Patton et al. 1994; Yones and McClay 2002). The Gulf of Suez is considered the most prolific oil province in Egypt, which is receiving the attention of many investigators due to the prospective potentials of hydrocarbon deposits that it attains. It constitutes a rift basin that was created by stretching and collapse of the crust. This process is often associated with hydrocarbon accumulation. Subsidence moves potential source rocks to depths suitable for oil and gas generation, and the stretching motion can produce structural traps in the fault blocks, which characterize rift basins (Schlumberger 1995).

The Gulf of Suez continues to provide a focal point for the development of geological ideas and evolution of oil-related technology. New companies are entering the area and bringing a variety of exploration techniques. Well logging and borehole seismic surveying data are among the most effective tools in use which are utilized for exploring and evaluating the hydrocarbon reservoirs. They can be integrated together to better understand the reservoir of interest. The respective contribution of integrating both techniques is reflected obviously on the quality of the information of both techniques (Lashin et al. 2011).

The study area is bounded between latitudes 27°50′N and 28°18′N, and longitudes 33°09′E and 33°40′E, southwestern Gulf of Suez, Egypt. It constitutes an area of about 55 km long and 45 km wide that covers the Morgan accommodation zone (MAZ), the southernmost part of the central Belayim dip province (BDP) and the northern part of the Amal-Zeit dip province (Fig. 1).

Many hydrocarbon traps producing oil from different reservoirs of different geological ages (Lower Cretaceous to the Miocene) are encountered in the Gulf of Suez. The Miocene-aged Asl and Hawara Formations are considered the main hydrocarbon reservoirs and source rock potentials in the southwestern part of the Gulf of Suez, including Morgan oil field (Schlumberger 1984, 1995). The aim of this paper is to (a) enhance a comprehensive petrophysical analysis of the upper part of the Rudeis Formation (Asl and Hawara Formations) that attains the most significant Miocene
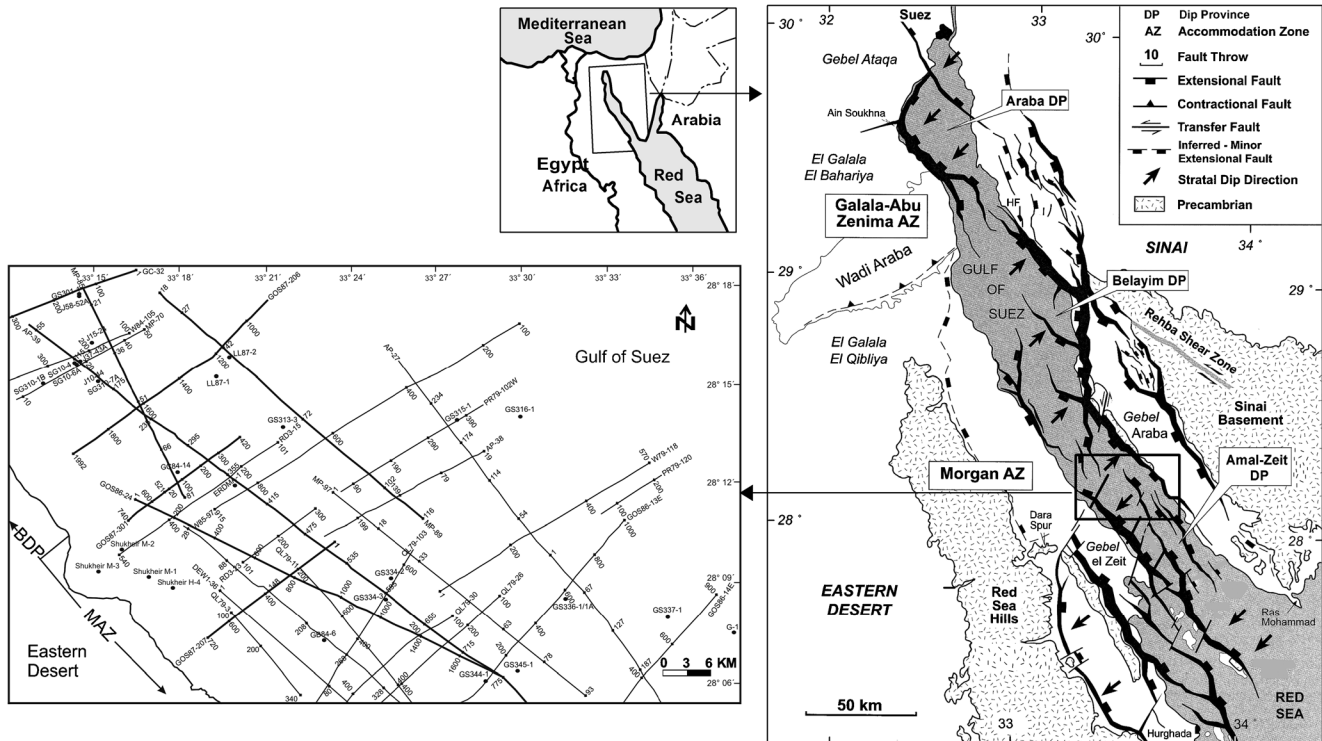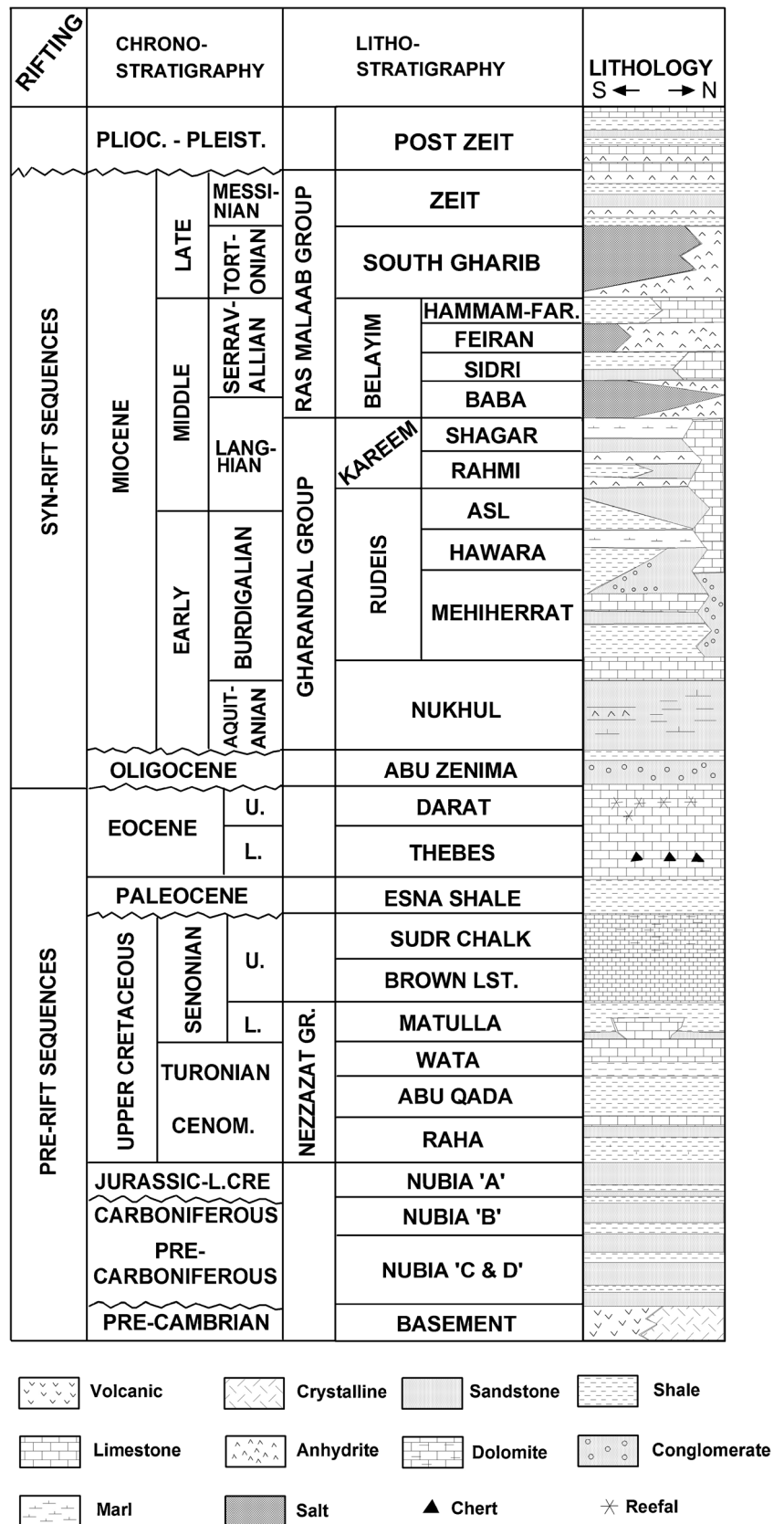

Fig. 1 Tectonic map of the Gulf of Suez rift (modified after Abd El-Naby et al. 2009). The shot point location map of the study area (*rectangle*, including location of the wells) is located in the southern Belayim dip province (BDP) and the northern Morgan Accumulation Zone (MAZ)

Fig. 2 Stratigraphic column of the Gulf of Suez (modified after Schlumberger 1995; El-Naby et al. 2010)

Legend:
- Volcanic
- Crystalline
- Sandstone
- Shale
- Limestone
- Anhydrite
- Dolomite
- Conglomerate
- Marl
- Salt
- Chert
- Reefal

reservoirs, (b) evaluate their hydrocarbon potentialities and (c) investigate the structural framework and its control on sequence stratigraphy of the syn-rift rocks.

Geologic setting

The geologic setting of the Gulf of Suez is a complex framework, dissected by a number of faults trending along N–S to NNE–SSW, E–W trending normal faults at the rift borders and within the rift basin and NE-trending strike-slip faults crossing the Gulf basin (Abd El-Gawad 1970; Bobbit and Gallagher 1978; Khalil 1984; Shahin and Shehab 1984; Hagras 1986; Meshref et al. 1976; 1988; Soliman 1988; Hataba et al. 1990; Rashed 1990; Shahin 1992; Hassouba et al. 1994; Shahin et al. 1994; Lashin and Abd El-Aal 2004; and El-Naby et al. 2009; 2010). The major fault systems are

mainly related to the tectonic and seismic activity of the Gulf of Suez and Red Sea region (Al Arifi et al. 2012). The interaction of these major fault systems resulted in a complex structural pattern consisting of numerous horsts and grabens with variable relief and dimensions. The Gulf of Suez is subdivided into three structural provinces according to their structural settings and regional dip directions: the northern Araba dip province (SW dips), the central BDP (NE dips) and the southern Amal-Zeit dip province (SW dips, Fig. 1). These provinces are separated by two NE-trending accommodation zones: the Galala-Abu Zenima accommodation zone (GAZAZ) in the north and the MAZ in the south (Harper 1966; Moustafa 1976; Bosworth 1985; Coffield and Schamel 1989; Gawthorpe and Hurst 1993; El-Naby et al. 2009).

Based on surface and subsurface data, the stratigraphic succession of the Gulf of Suez can be subdivided into three depositional units (Fig. 2). The pre-rift units include Proterozoic

Fig. 3 Location map shows the distribution of the studied wells throughout the study area
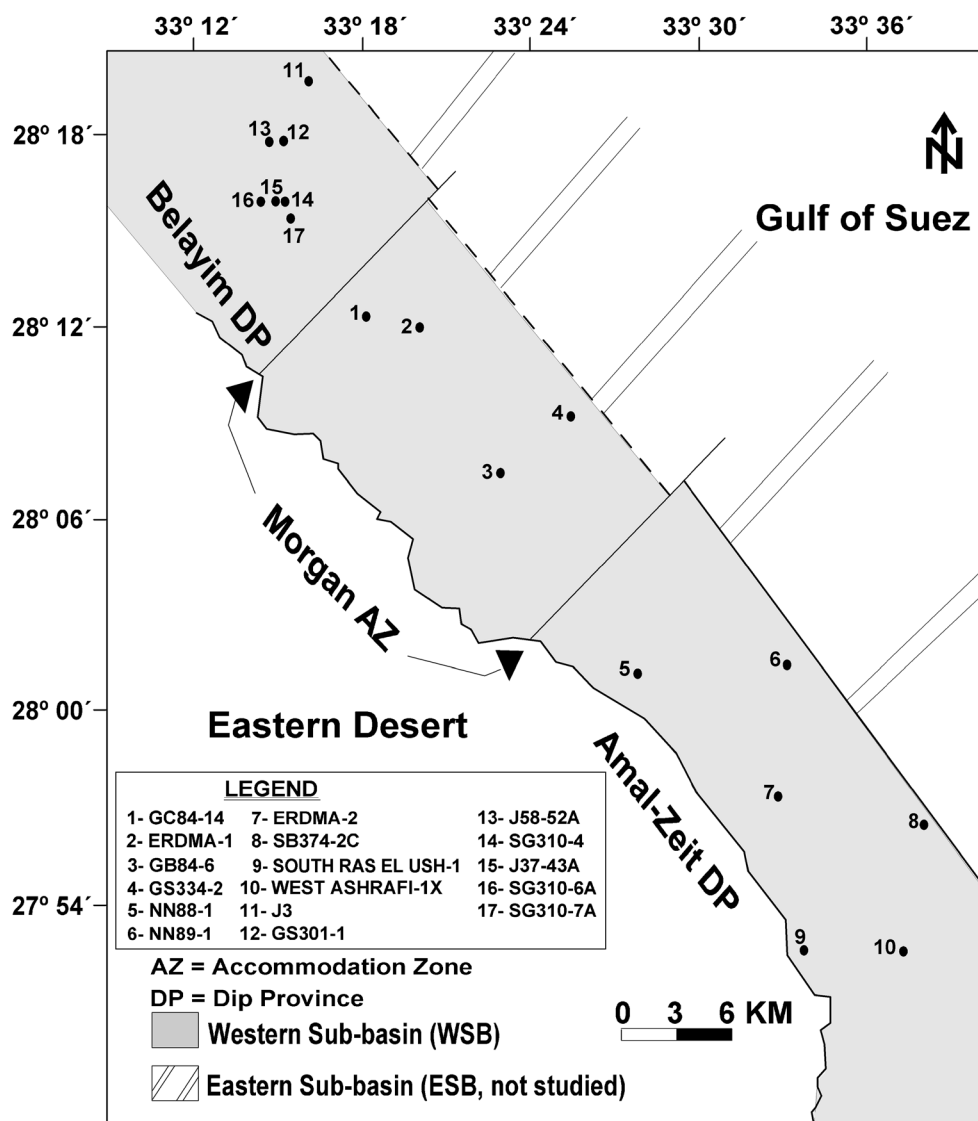
basement rocks and Paleozoic to Upper Eocene sediments. These formations are important as source and reservoir rocks. The Upper Oligocene and Miocene syn-rift units contain source, reservoir and seal lithologies, as well as volcanic rocks. The post-rift units are of Pliocene to Pleistocene age. The Miocene rocks are of prime interest as they encounter two important formations (Asl and Hawara) which are considered the main oil-bearing reservoirs in the southern part of Gulf of Suez. Asl and Hawara Formations together with Mheiherrat Formation are equivalent to Rudeis Formation. These two formations are composed of clastic lithology (mainly sandstones) in the northern part of the study area and proved to have prospective sand reservoirs of good hydrocarbon potentiality (Lashin et al. 2011; Lashin and Mogren 2012; Lashin and Serag El Din 2012). In the southern part of the study area, the composition of Asl and Hawara Formations tends to be calcareous in lithology with considerable hydrocarbon potentiality (El-Naby et al. 2010).

Datasets and methodology

The aim of this work is to study the petrophysical characteristics and hydrocarbon potentiality of the Asl and Hawara Formations in East Morgan oil field, Gulf of Suez, Egypt, as well as investigating the seismic structural and seismic facies features of these formations. The different logging datasets (resistivity logs, neutron, density, gamma ray, calliper, etc.) of 17 wells scattered in the study area and the 2D seismic sections of 27 seismic profiles dissecting East Morgan oil field are all used for achieving this purpose (Fig. 3).

The petrophysical analysis is basically based on the logging data of GC 84–14, ERDMA-1, GB84-6, GS334-2, NN88-1, NN89-2, ERDMA-2, SB374-2C, South Ras El Ush-1, West Ashrafi-1X, J3, GS301-1, J58-52A, SG310-4, J37-43A, SG310-6A and SG310-7A wells. A PC-based visual basic programme is used in performing the primary processing and corrections of data. A clastic sand petrophysical module is used for analysing the reservoirs in the northern part of the study area (BDP), while another petrophysical carbonate module is used for the reservoirs in the middle (MAZ) and southern part of the study area. The petrophysical analysis is concerned with deducing the main parameters that are necessary for reservoir characterization and hydrocarbon potentiality evaluation. These parameters include the lithological constituents, rock total and effective porosities, shale volume, water and hydrocarbon saturations, etc. A number of petrophysical plots and property maps are constructed for the main petrophysical parameters of the reservoir of interest to illustrate their distribution in the study area both vertically and laterally.

Table 1 The average deduced petrophysical parameters with respect to 11 representative wells in the study area

| No.	Wells	Formation	Top (ft.)	Bottom (ft.)	Φ TOT. (fr)	Φ EFF. (fr)	VSH (fr)	SW (fr)	SH (fr)
1	GB 84-6	Asl	10,920	11,480	0.20	0.04	0.52	0.95	0.05
		Hawara	11,480	11,768	0.26	0.09	0.49	0.98	0.02
2	GC 84-14	Asl	10,335	10,512	0.20	0.10	0.53	0.91	0.09
		Hawara	10,512	10,603	0.17	0.06	0.55	0.98	0.02
3	ERDMA-1	Asl	8,531	10,483	0.21	0.10	0.29	0.97	0.03
		Hawara	10,550	11,572	0.18	0.08	0.21	0.96	0.04
4	GS 334-2	Asl	7,734	8,100	0.20	0.09	0.45	0.88	0.12
		Hawara	8,100	8,336	0.19	0.08	0.50	0.95	0.05
5	J37-43A	Asl	10,406	10,740	0.15	0.01	0.67	1.0	0.0
		Hawara	10,740	11,000	0.14	0.04	0.41	0.76	0.24
6	SG 310-7A	Asl	11,270	11,350	0.14	0.03	0.47	0.89	0.11
		Hawara	11,350	11,600	0.16	0.06	0.49	0.68	0.32
7	GS 310-6A	Asl	13,150	13,848	0.14	0.09	0.23	0.52	0.48
		Hawara	13,848	14,652	0.13	0.09	0.20	0.81	0.19
8	SG 310-4	Asl	10,801	11,080	0.14	0.04	0.49	0.80	0.20
		Hawara	11,080	11,600	–	–	–	–	–
9	J3	Asl	8,863	9,320	0.25	0.0	0.89	0.98	0.02
		Hawara	9,320	9,790	0.31	0.0	0.99	1.0	0.0
10	GS 301-1	Asl	13,484	13,684	0.15	0.05	0.18	0.64	0.36
		Hawara	13,684	14,002	0.20	0.01	0.70	0.94	0.06
11	J58-52A	Asl	8,630	8,940	0.16	0.05	0.36	0.84	0.16
		Hawara	8,940	9,250	0.21	0.0	0.60	1.0	0.0
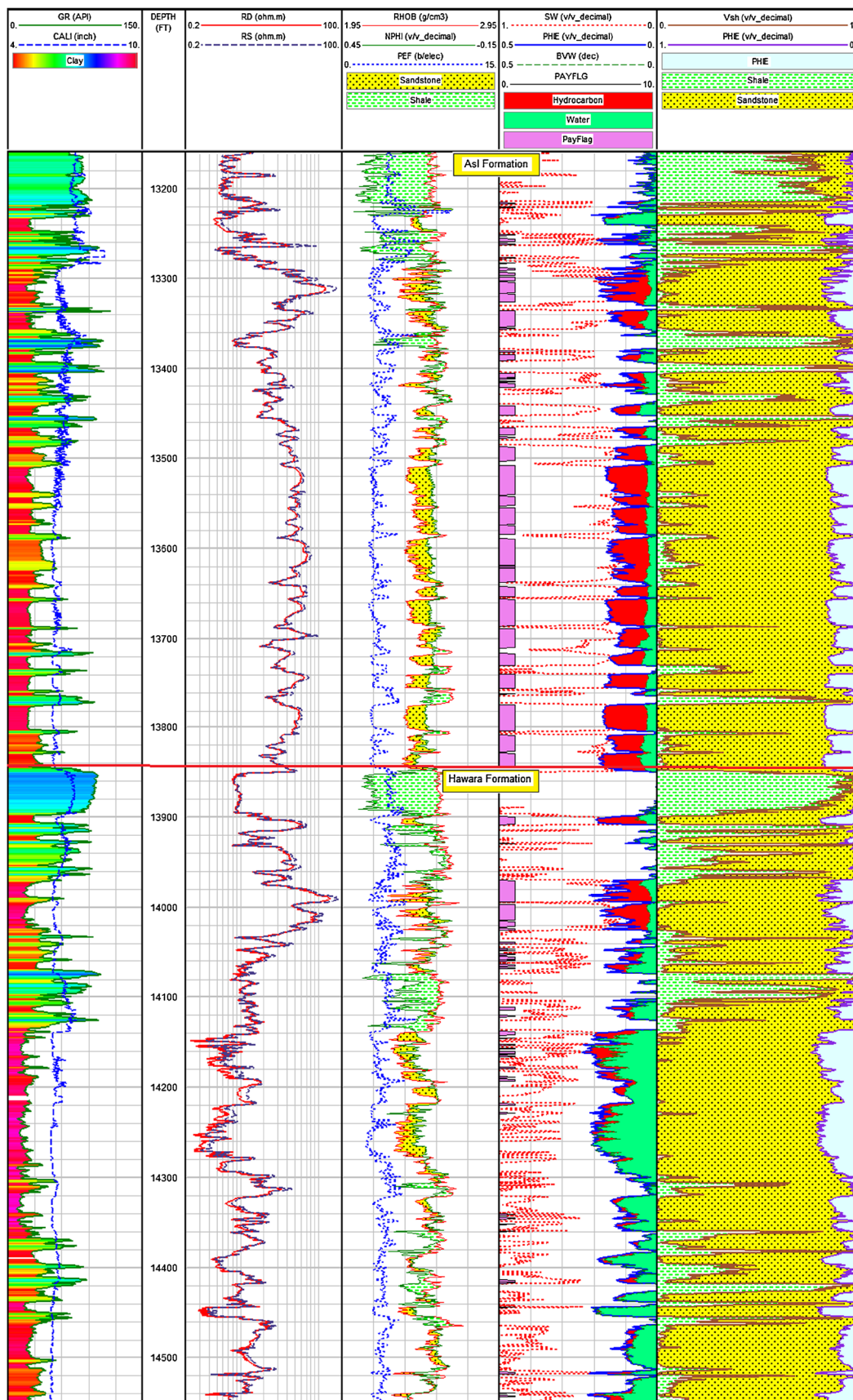
Fig. 4 Petrophysical data log of GS310-6A well, East Morgan oil field, Gulf of Suez

The seismic data analysis is mainly based on the interpretation of the 2D seismic sections, their velocity logs and vertical seismic profiles (VSP), as well as the available lithologic logs. A number of geo-seismic cross sections are constructed and interpreted to investigate the structural setting of the study area and clarify the main structural elements that affect the hydrocarbon-bearing reservoir.

The information obtained from the petrophysical interpretation of well data, seismic velocity analysis and structural investigation were integrated to delineate the different depositional sequences, their boundaries and seismic facies characteristics in the studied Miocene succession according to Vail et al. (1977a, b), Vail (1987), Wagoner et al. (1988; 1990), Posamentier and Weimer (1993) and Emery and Myers (1996). The procedures followed in the seismic stratigraphic analysis are based mainly on dividing the seismic sections into discrete depositional sequences that make up the studied Miocene succession. These sequences are bounded

above and below by definite sequence boundaries (Emery and Myers 1996). The main steps usually used in sequence stratigraphy and seismic facies analysis are (a) separating time-depositional units based on detecting unconformities or changing in seismic patterns, (b) tracing these unconformities in the different seismic sections to trace the sequence boundaries, (c) seismic facies analysis, and (d) determining depositional environments from seismic reflection characteristics.

Petrophysical analysis

The petrophysical and hydrocarbon characteristics of Asl and Hawara formations are based mainly on the well logging analysis of 17 wells, which are distributed along the northern part of the MAZ and the southernmost part of BDP (Fig. 3). This area reflects the northern part of the studied western sub-basin (WSB; compare Fig. 1). A number of petrophysical
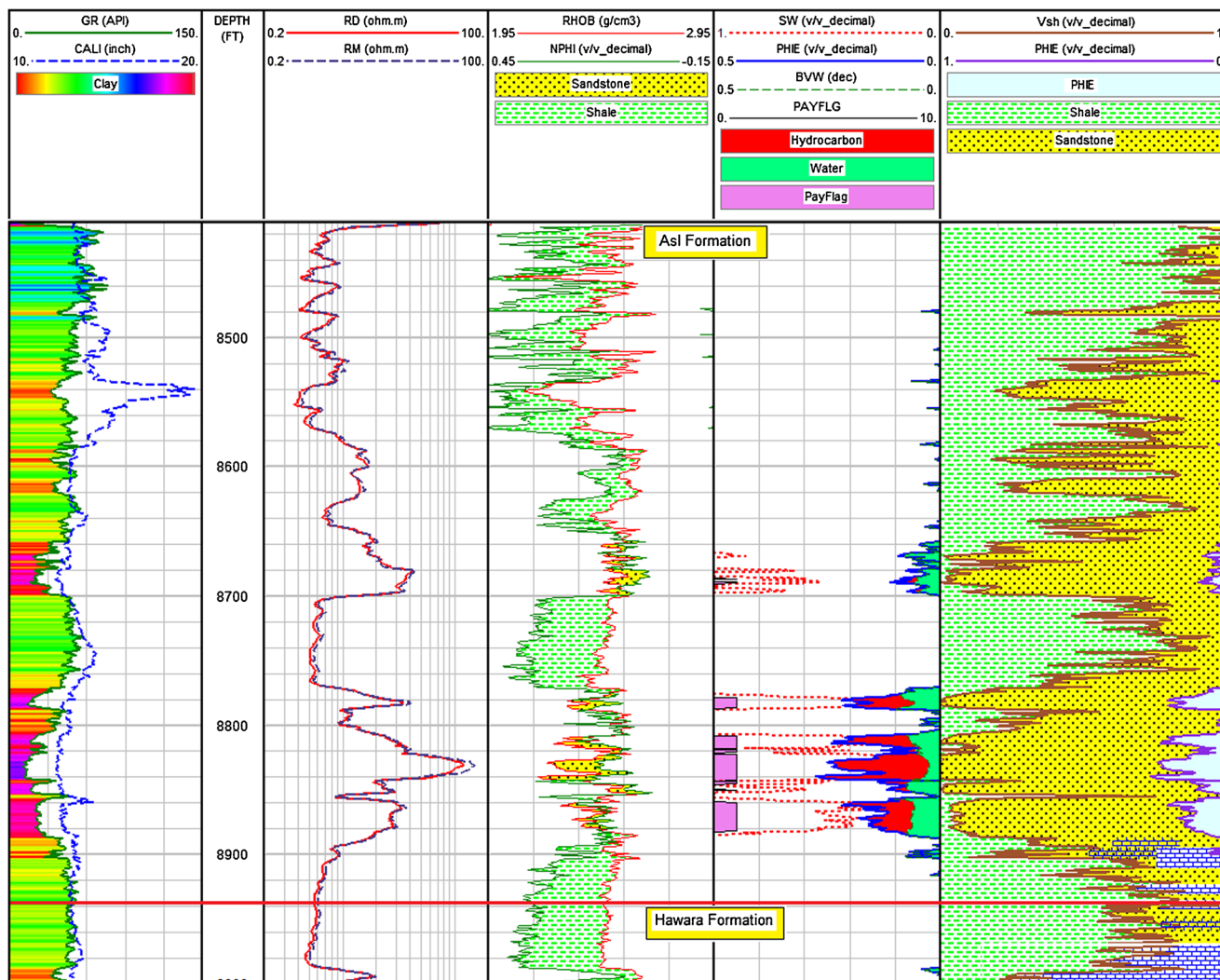

Fig. 5 Petrophysical data log of J85-52A well, East Morgan oil field, Gulf of Suez

plots are constructed for the studied wells. These plots are the final layout that collect the different deduced petrophysical parameters, of prime interest, together and allow their interpretation vertically with depth. Additionally, a number of distribution maps are constructed for Asl and Hawara sand reservoirs such as total porosity, effective porosity, volume of shale, water saturation and hydrocarbon saturation maps.

Vertical distribution of petrophysical parameters

Table 1 summarizes the average values of the different deduced petrophysical parameters of some representative wells in the study area. Figures 4, 5, 6, 7, 8 and 9 represent the petrophysical data logs of six selected wells (GS310-6A, J85-52A, GS 301–1, GC 84–14, ERDMA-1 and GS334-2) distributed in the MAZ and BDP.

The petrophysical data log of GS310-6A well is represented in Fig. 4. This well is the most important among all the studied wells that are located at the southernmost part of

the BDP (south of the J85-52A well). Asl Formation in this well exhibits excellent petrophysical characters in the form of very low shale content, good pore spaces and high hydrocarbon saturation. Porosity pattern is irregular and tends to decrease upward. Such pore spaces (13 %) are mainly saturated with hydrocarbon (82 %), and the remainder is water (18 %). Unlike Asl Formation, Hawara Formation is characterized by high content of water on the expense of the hydrocarbon. The upper part of the formation (13,900–14,100 ft.) is more enriched by hydrocarbon than the lower part. Petrophysical values of 13 %, 81 % and 19 % are recorded for effective porosity, hydrocarbon and water saturations, respectively. In general, shale volume is low, and pore spaces are irregular in pattern and increase obviously at the middle of the formation (at depth range of 14,140–14,300 ft.).

J85-52A well is another well located at the southernmost part of the BDP. Figure 5 shows the petrophysical data log of this well, where the interested Asl sand reservoir is encountered at a depth range of 8,775 and 8,885 ft. The effective
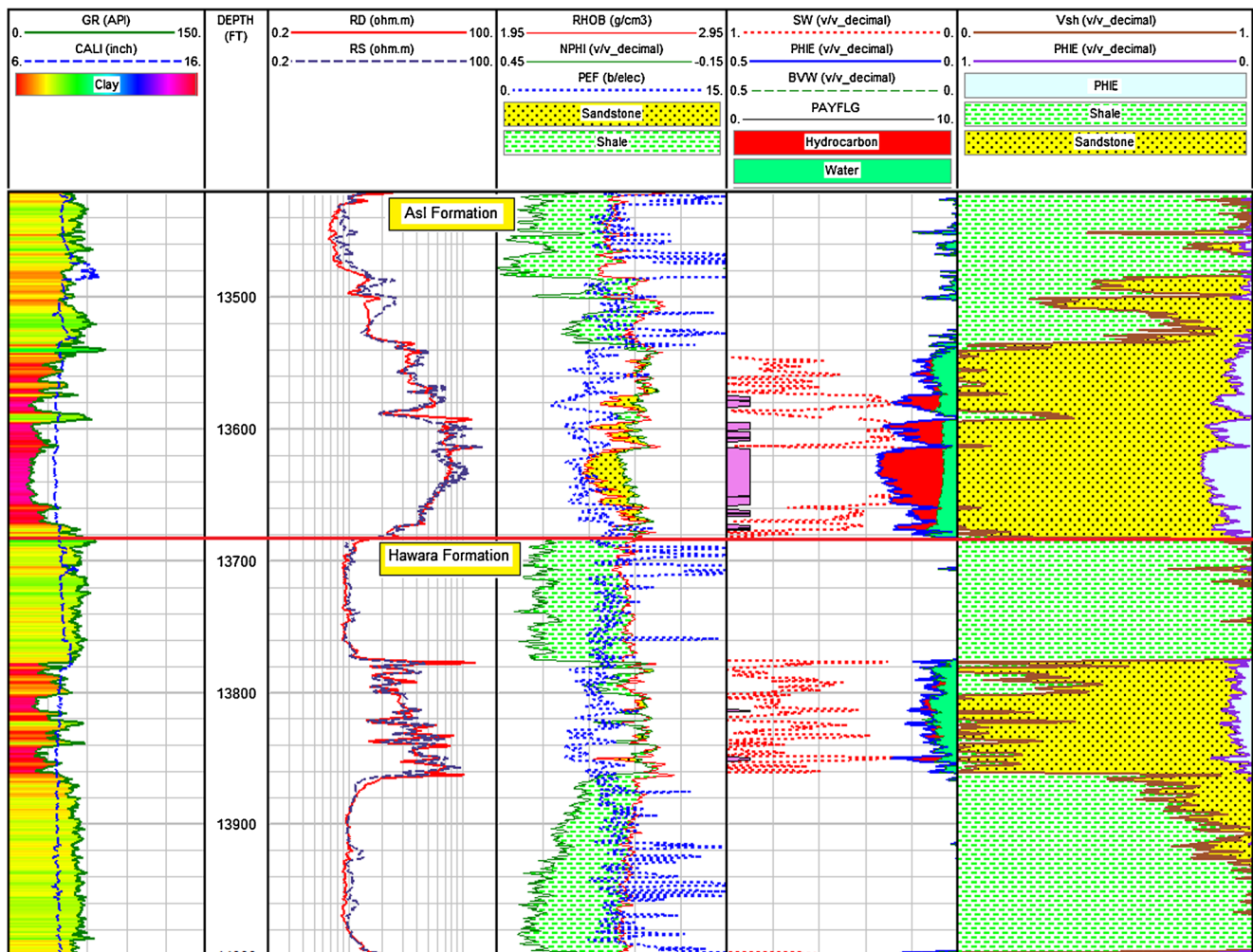

Fig. 6 Petrophysical data log of GS301-1 well, East Morgan oil field, Gulf of Suez
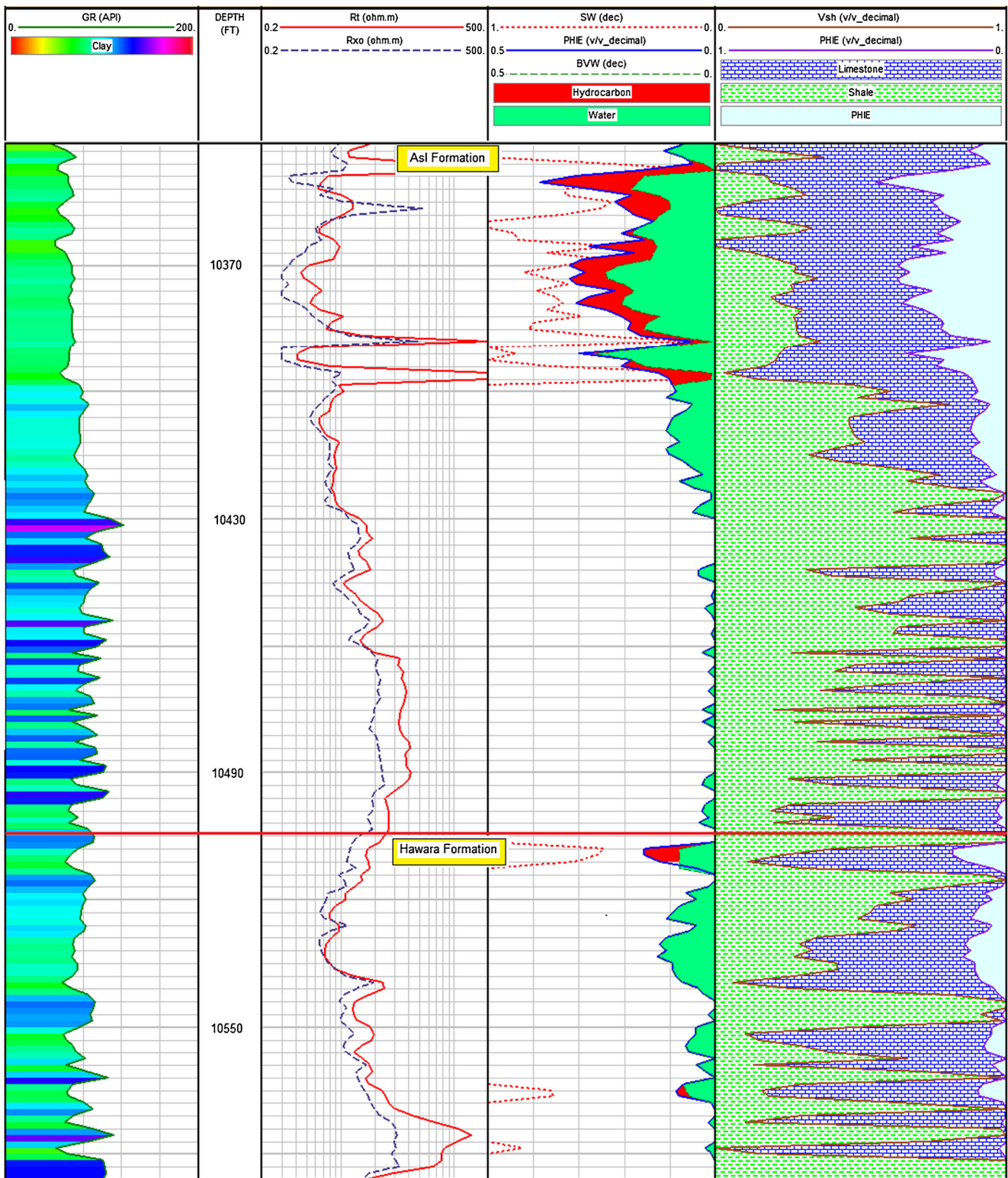
Fig. 7 Petrophysical data log of GC 84–14 well, East Morgan oil field, Gulf of Suez

porosity of this zone is relatively high (20 %), irregular in pattern and mainly saturated with hydrocarbon (70 %) and less water (30 %). Shale volume is very low in front of this zone (10 %) and increases apparently (75 %) in the overlying and underlying parts of the section. These shale-enriched zones exhibit irregular pore spaces (7.5 %) and mainly
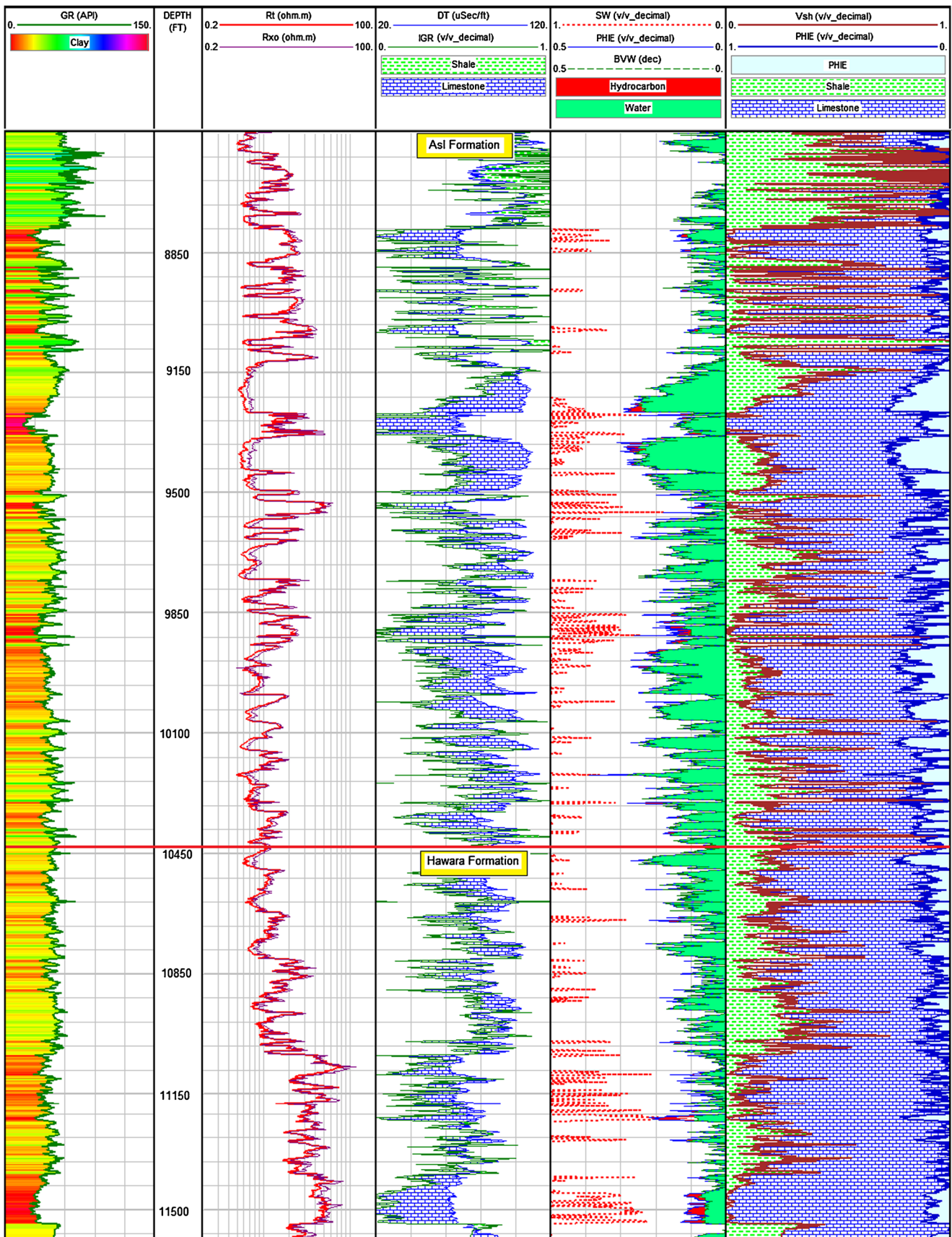
Fig. 8 Petrophysical data log of ERDMA-1 well, East Morgan oil field, Gulf of Suez
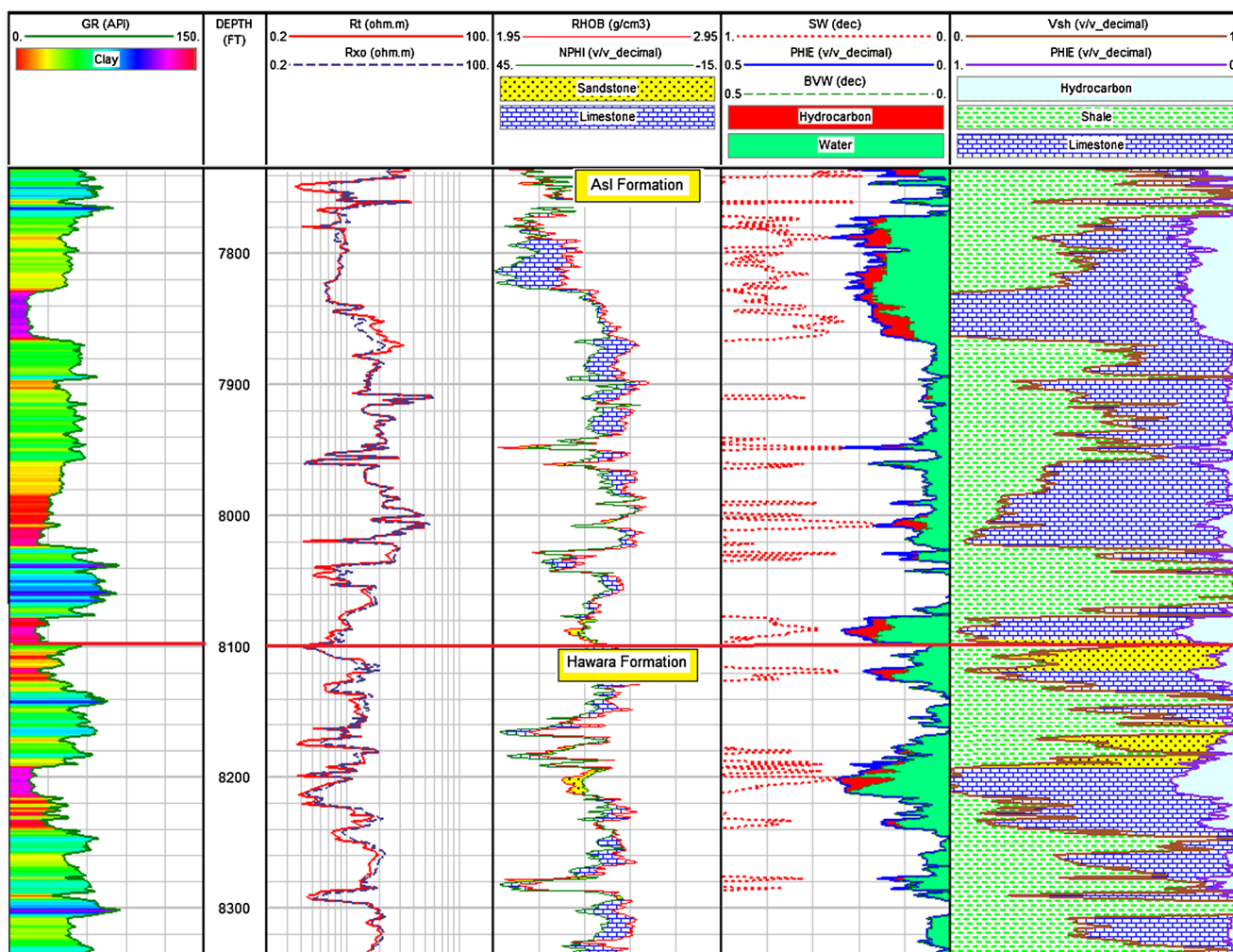
Fig. 9 Petrophysical data log of GS334-2 well, East Morgan oil field, Gulf of Suez

occupied by water. Hawara Formation, on the other hand, attains very poor petrophysical and hydrocarbon characteristics (very low pore spaces <5 % and high water content >95 %). It is not penetrated completely in this well, so it is represented by thin thicknesses (60 ft.) and composed mainly of shale with a few sand streaks which are calcareous in matrix.

Figure 6 shows the petrophysical data log of GS 301–1 well. An outstanding oil-bearing sand section (13,560–13,680 ft.) is detected at the lower part of Asl Formation. Very good average petrophysical parameters (low shale volume, 8 % and high effective porosity, 15 %) and high hydrocarbon content (64 %) are represented by Asl oil section, in this well. Hawara Formation, on the other hand, is characterized by the dominance of shale lithology (70 %) and high water content (94 %).

A unique lateral variation change of the facies of Asl Formation is presented in GC 84–14 well which is located at the extreme northern part of the MAZ (Fig. 7). The upper part

of Asl Formation (top of section to depth of 10,400 ft.) in this well is mainly composed of limestone lithology with varying proportions of shale. This zone exhibits irregular distribution of pore spaces (20 %) and considerable hydrocarbon content (28 %). The lower part of Asl Formation, on the other hand, consists mainly of shale which is calcareous in matrix, very low pore spaces (>3 %) and high water content. Hawara Formation exhibits irregular pore spaces mainly occupied by water (95 %) and poor hydrocarbon potentiality. It composed nearly of equal proportions of shale and limestone.

ERDMA-1 well is another well that is located at the northern part of the MAZ, more closely to GC 84–14 well (Fig. 8). Asl Formation is composed mainly of limestone with shale intercalations. Pore spaces are extremely irregular and increase obviously at the middle part of the formation (20 %). Water content is more than 95 %, and shale volume is relatively high (30 %). Hawara Formation consists mainly of limestone with little shale content. Pore spaces are low (7 %) and filled mainly with water.
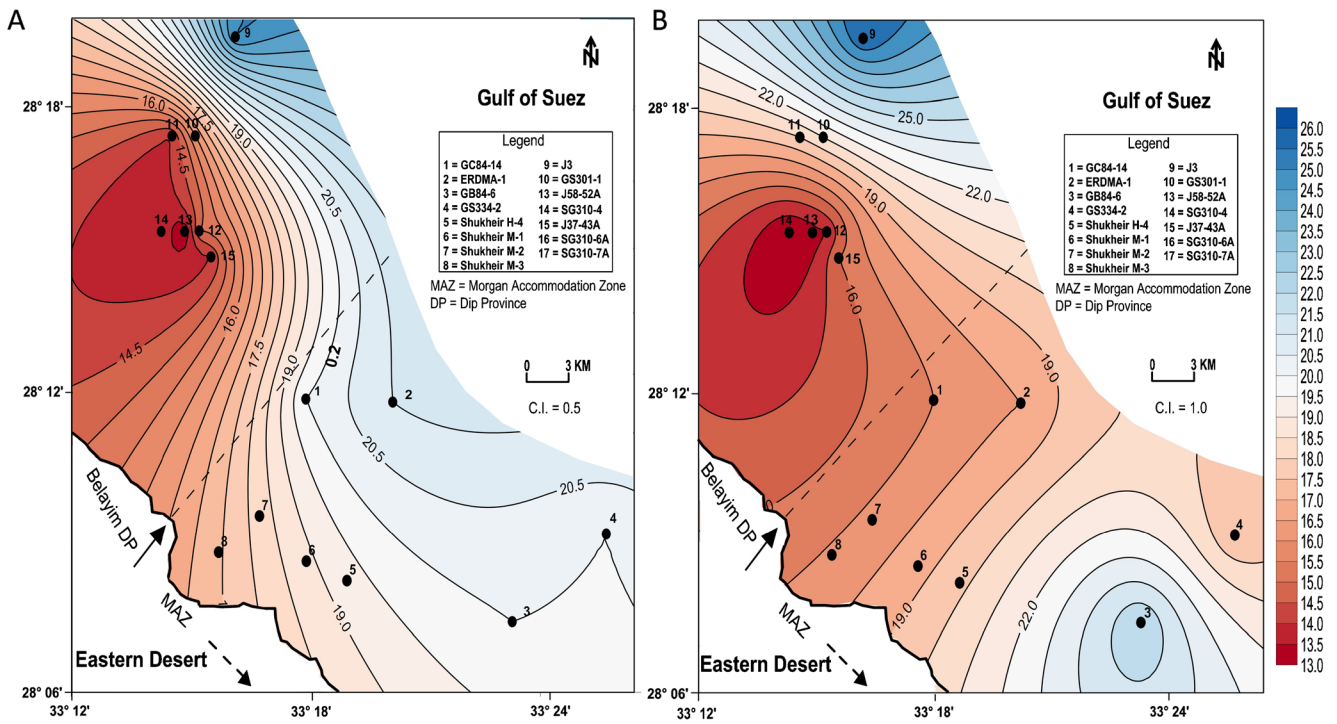
Fig. 10 Total porosity distribution maps of (**a**) Asl Formation and (**b**) Hawara Formation, East Morgan oil field, Gulf of Suez

The petrophysical data log of GS334-2 well (Fig. 9) is similar to that of ERDMA-1 well. Asl Formation is composed of alternative interactions of shale and limestone. Pore spaces are irregular, apparently increase (20 %) at the upper part of formation (depth range, 7,770–7,870 ft.) and mainly filled with water content (88 %). Nearly similar petrophysical characteristics are exhibited by Hawara Formation.
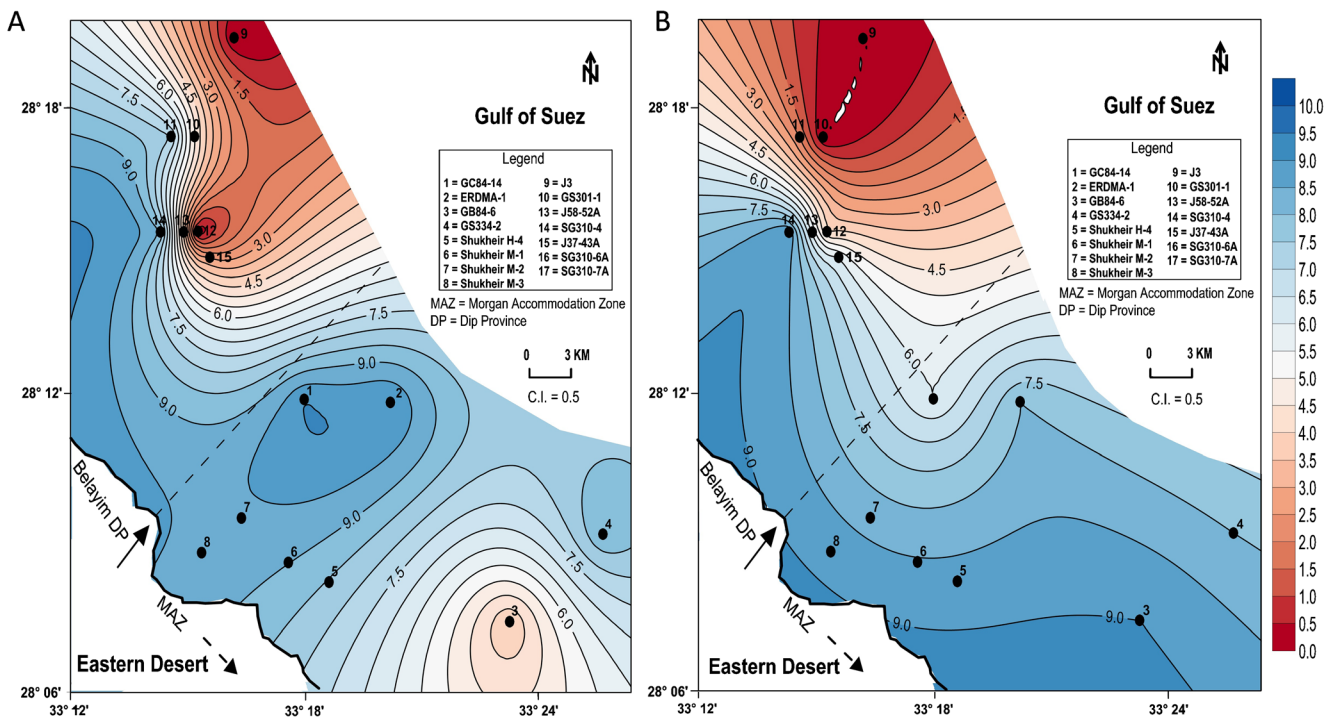

Fig. 11 Effective porosity distribution maps of (**a**) Asl Formation and (**b**) Hawara Formation, East Morgan oil field, Gulf of Suez
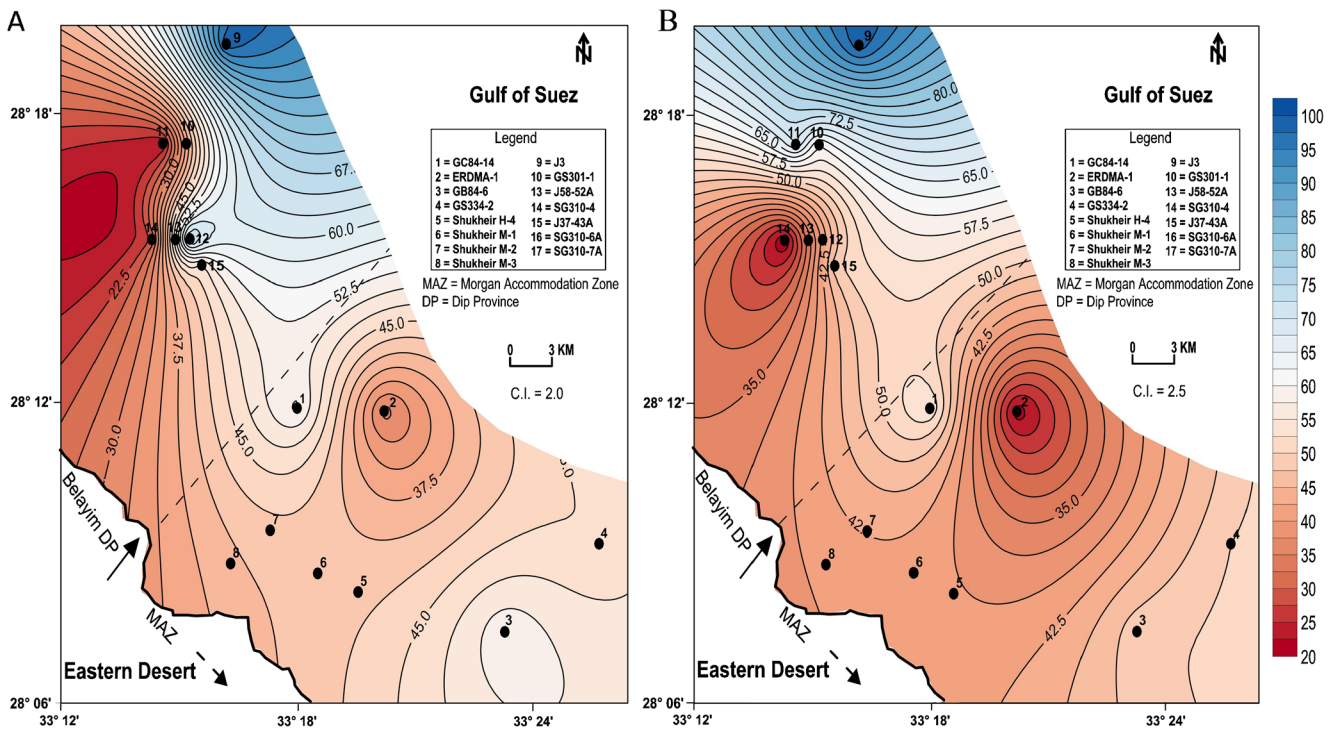
Fig. 12 Shale volume distribution maps of (a) Asl Formation and (b) Hawara Formation, East Morgan oil field, Gulf of Suez

It is worth to mention here that there is a remarkable change in the facies of Asl and Hawara formations from the dominance of the clastic sandstone lithology in the southern part of the BDP to the more calcareous lithology (limestone, shale intercalations and a few thin sandstone beds) at the northern part of the MAZ zone. Such increasing of sandstone lithology is associated with an increase of hydrocarbon content. In general, Asl Formation is more saturated with hydrocarbon as compared with Hawara Formation.
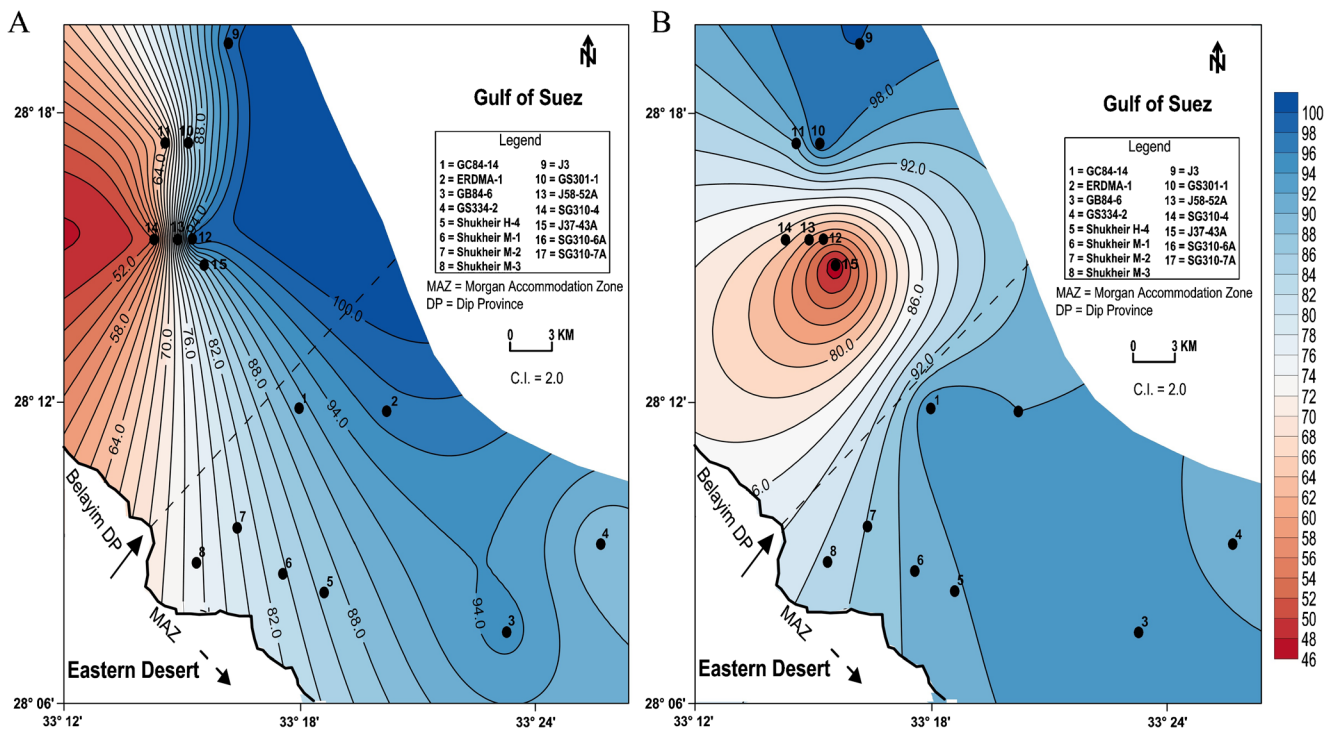

Fig. 13 Water saturation distribution maps of (a) Asl Formation and (b) Hawara Formation, East Morgan oil field, Gulf of Suez
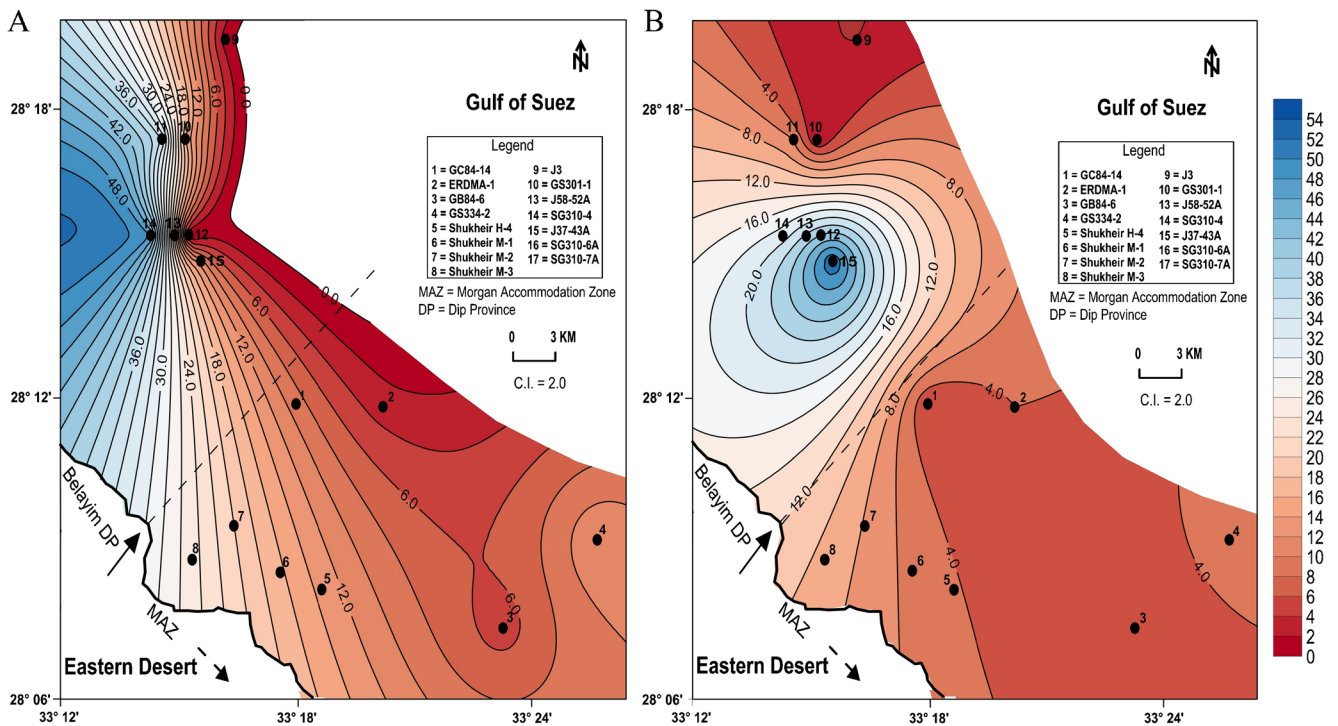
Fig. 14 Hydrocarbon saturation distribution maps of (a) Asl Formation and (b) Hawara Formation, East Morgan oil field, Gulf of Suez

Lateral distribution of petrophysical parameters

Lateral distribution of the petrophysical parameters of interest was enhanced in the present study, especially for those parameters concerning with hydrocarbon potentialities.

Accordingly, a number of property distribution maps were constructed for Asl and Hawara sand reservoirs such as total porosity, effective porosity, volume of shale, water saturation and hydrocarbon saturation maps (Figs. 10, 11, 12, 13 and 14).
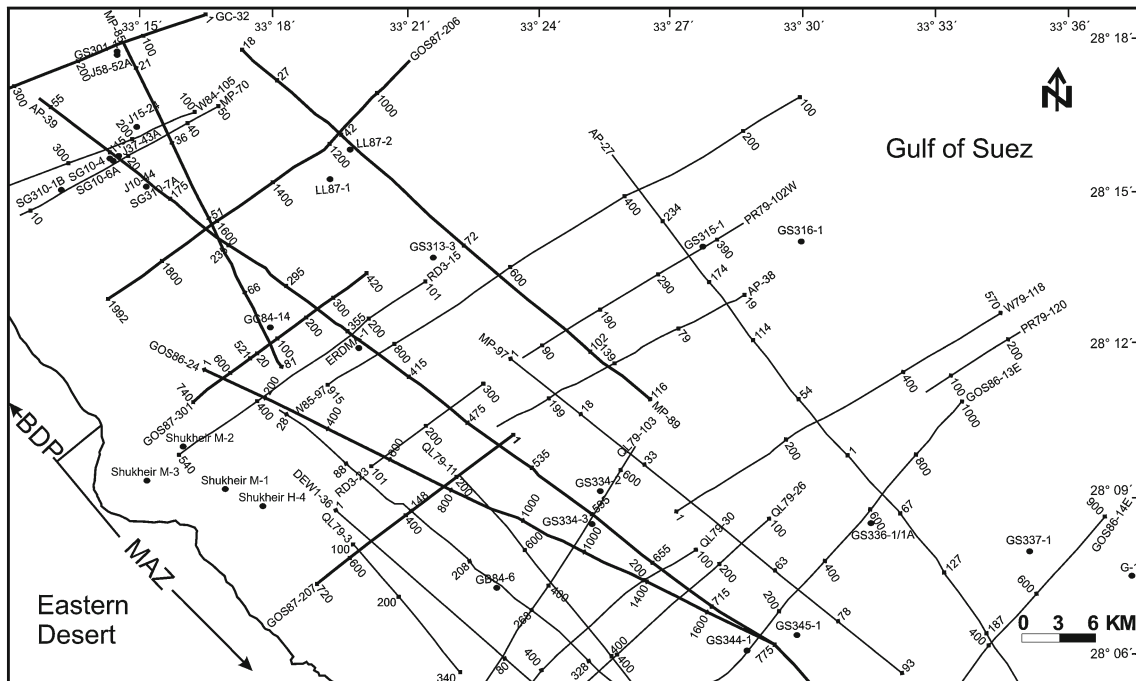

Fig. 15 Shot point location map of the study area

Table 2 Summary of the details of seven selected seismic sections in the study area

No.	Seismic section	Start	End	Direction	Length (km)	Processing
1	GC 32	Long. 33°12′20″E Lat. 28°16′25″N	Long. 33°15′38″E Lat. 28°18′06″N	NE–SW	16.5	Geophysical Company of Norway 'GECO' 1978
2	GOS 87-206	Long. 33°14′21″E Lat. 28°12′56″N	Long. 33°21′03″E Lat. 28°17′38″N	NE–SW	30.6	Compagnie Générale de Géophysique 'CGG' 1988
3	AP 39	Long. 33°13′02″E Lat. 28°16′03″N	Long. 28°05′35″E Lat. 33°30′01″N	NW–SE	63	Western Geophysical 1969
4	MP 89	Long. 33°17′16″E Lat. 28°12′58″N	Long. 33°26′41″E Lat. 28°11′02″N	NW–SE	44	Western Geophysical 1965
5	GOS 86-24	Long. 33°16′05″E Lat. 28°11′04″N	Long. 33°29′15″E Lat. 28°06′10″N	NW–SE	52	Compagnie Générale de Géophysique 'CGG' 1987
6	GOS 87-301	Long. 33°16′00″E Lat. 28°10′02″N	Long. 33°20′17″E Lat. 28°13′18″N	NE–SW	18	Compagnie Générale de Géophysique 'CGG' 1987
7	GOS 87-207	Long. 33°19′02″E Lat. 28°07′30″N	Long. 33°22′23″E Lat. 28°10′09″N	NE–SW	20	Compagnie Générale de Géophysique 'CGG' 1987

Total porosity distribution maps

Figure 10a shows the total porosity distribution map of Asl sand reservoir. This map indicates gradual increasing of the values towards the northeast of the WSB. The maximum porosity value of 25 % is represented by J3 well at the northernmost part of the BDP. Porosity values decrease towards the southwest direction constituting a semi-closure represented by J85-52A, SG310-4, J37-43A, SG310-6A and SG310-7A wells. The minimum total porosity recorded for Asl sand at these wells is 14 %.

The total porosity distribution map of Hawara Formation shows a similar response to that of the Asl Formation in the upper part of the study area, in terms of the northeast increase and the southwest decrease of values (Fig. 10b). In the lower part of the map, porosity values tend to increase to the

southeast constituting a semi-closure centred by GB84-6 well (26 %).

Effective porosity distribution maps

The effective porosity map of Asl Formation is represented in Fig. 11a. Regarding the map, one high porosity semi-closure is recognized in the middle (9 %, occupied by wells 1, 2, 6, 7 and 8), besides another low porosity semi-closures in the northwest and southeast. In general, porosity values increase to the northwest and west directions of the WSB (in the southernmost part of the BDP), while they decrease to the north, northeast and south directions. Figure 11b shows the effective porosity map of Hawara Formation. Porosity values increase gradually to the south, west and southwest directions, where a maximum recorded value of 9 % is represented by

Fig. 16 Interpreted seismic section GC 32, East Morgan oil field, Gulf of Suez
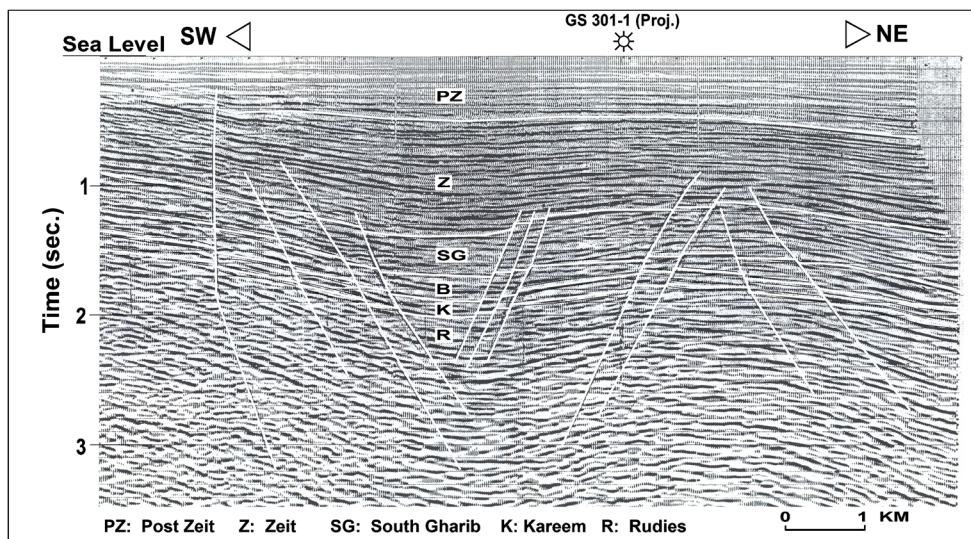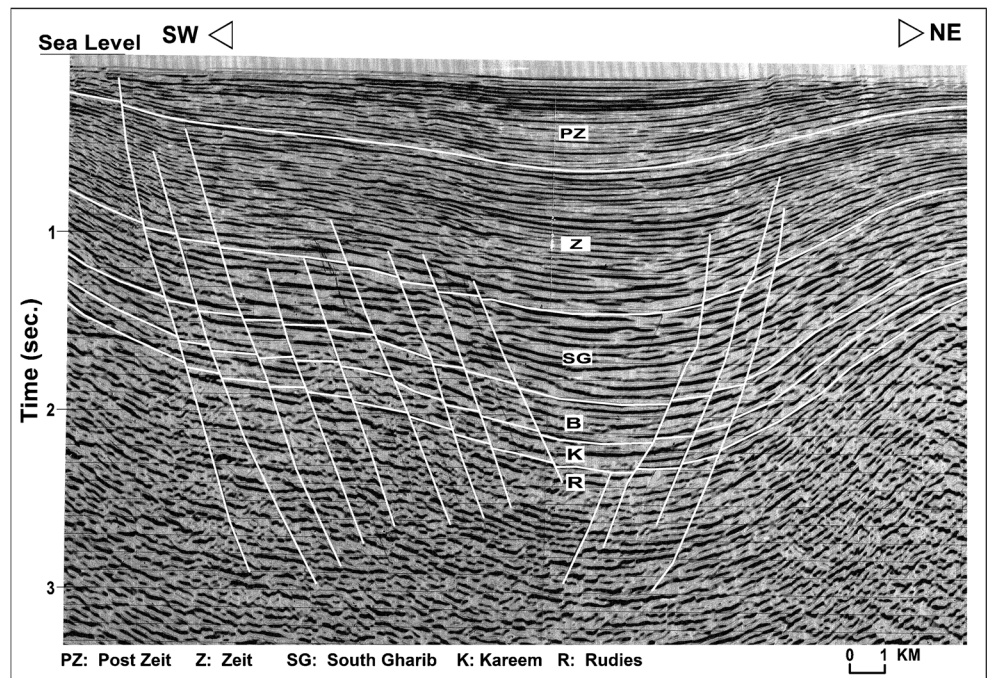
Fig. 17 Interpreted seismic section GOS 87–206, East Morgan oil field, Gulf of Suez

GB84-6 well. To the north and northwest directions, the porosity diminishes gradually until it reaches the value of 1 % (GS301-1 well).

Shale volume distribution maps

Figure 12a exhibits the volume of shale distribution map of Asl Formation. Generally, the volume of shale values increases along a northeast direction (Vsh=80 % at J3 well), where a remarkable decrease of effective porosity is observed (see Fig. 11a). The lowest recorded shale volume value (20 %) is recorded to the west of the BDP zone. Two closures of shaly nature are observed in the middle of MAZ

zone around ERDMA-1 well (29 %) and in the extreme southeastern part of the area (50 %). The volume of shale distribution map of Hawara Formation (Fig. 12b) is quite similar to that of Asl Formation, reflecting similar effect on the effective porosity. The maximum shale volume value (99 %) is recorded at the northern part (J3 well), while the lowest recorded value (21 %) is given by ERDMA-1 well in the middle of the MAZ zone.

Water saturation distribution maps

Regarding the water saturation map of Asl Formation (Fig. 13a), it appears clear that water saturation increases to

Fig. 18 Interpreted seismic section AP 39, East Morgan oil field, Gulf of Suez
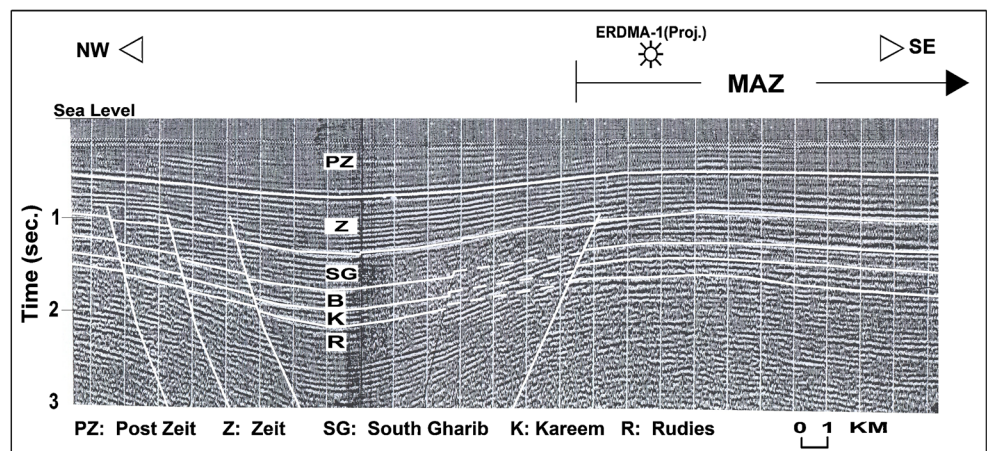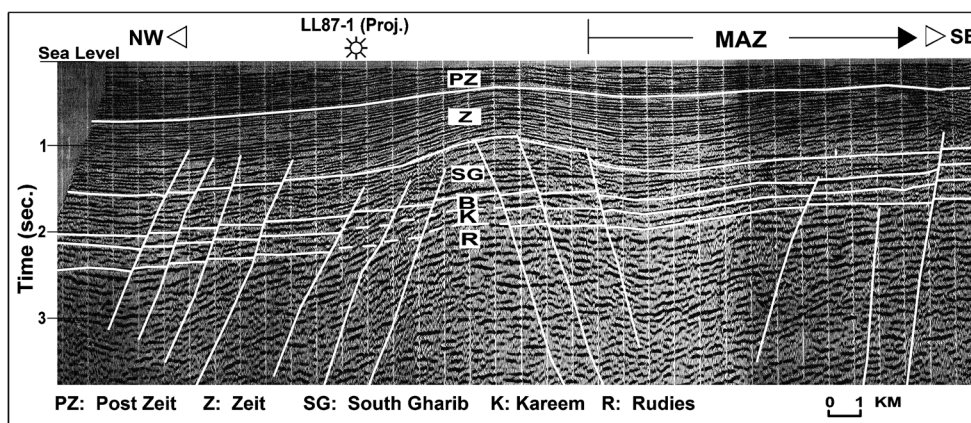
Fig. 19 Interpreted seismic section MP, East Morgan oil field, Gulf of Suez

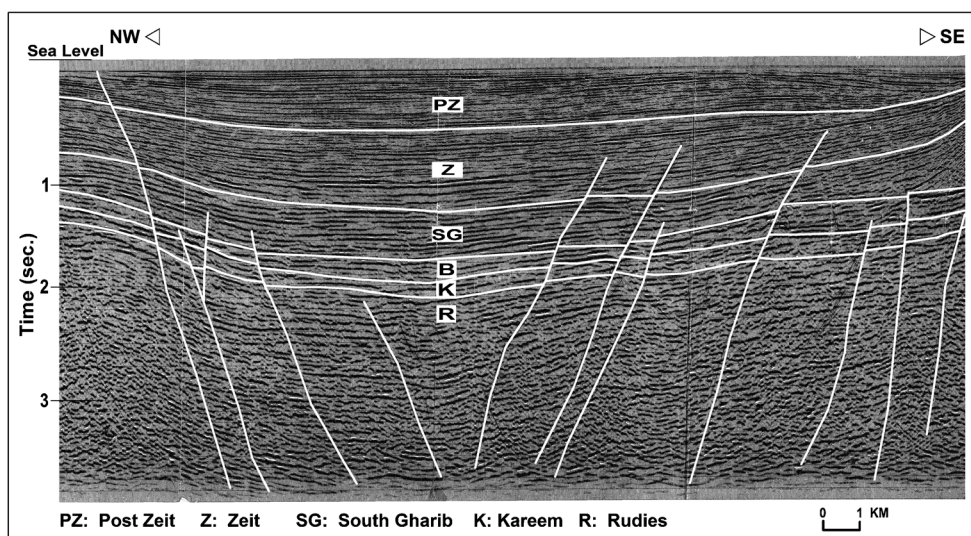PZ: Post Zeit   Z: Zeit   SG: South Gharib   K: Kareem   R: Rudies

the northeast and the southeast directions with a maximum value of 98 % at J3 well. The minimum value (52 %) is recorded at the western middle part of MAZ. The water saturation map of Hawara Formation (Fig. 13b) shows a good closure of low water content at the middle of the BDP zone. Water saturation reaches its minimum value at the centre of this closure (72 %), while a maximum value of 100 % is recorded at the north (J3 well).

Hydrocarbon saturation distribution maps

The hydrocarbon saturation distribution maps of Asl and Hawara Formations exhibit a similar reverse response to that of the water saturation. The hydrocarbon saturation decreases to the northeast and southeast and increases to the west in case of Asl Formation (Fig. 14a). Meanwhile, for Hawara Formation, a good hydrocarbon saturation (30 %) is recognized at the centre of the closure located at the middle of the MAZ zone (Fig. 14b).

Seismic interpretation

The interpretation of the structural setting, sequence definition and seismic facies of the study area is based on the interpretation of 27 2D seismic profiles (Fig. 15) and the available composite logs of wells.

Seismic structural analysis

Among the 27 interpreted seismic profiles, seven sections were selected to demonstrate and illustrate the structural framework of the study area. Table 2 summarizes the details of these seismic sections.

Seismic section GC 32

Figure 16 shows the 2D interpreted seismic section GC 32 passing through the northern part of the study area (at southern part of the BDP) and running parallel to line GOS 87–

Fig. 20 Interpreted seismic section GOS 86–24, East Morgan oil field, Gulf of Suez

PZ: Post Zeit   Z: Zeit   SG: South Gharib   K: Kareem   R: Rudies

Fig. 21 Interpreted seismic section GOS 87–301, East Morgan oil field, Gulf of Suez
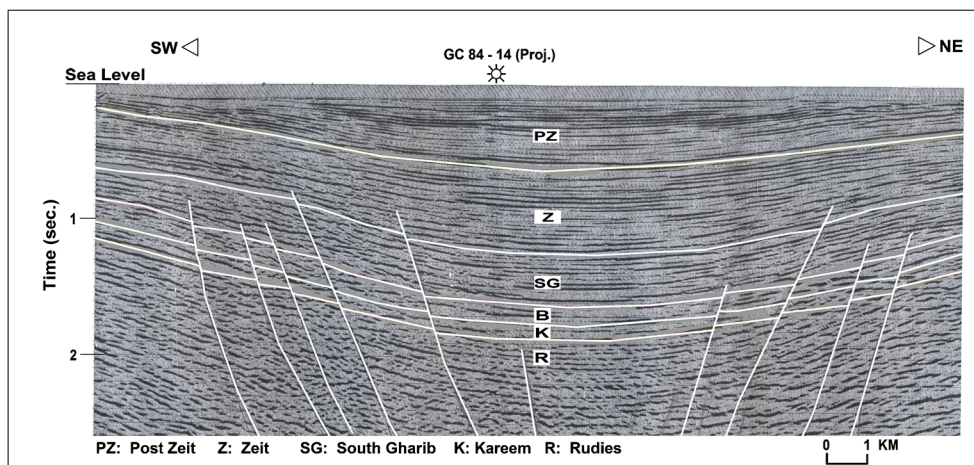
206 (Fig. 15). This section reveals the prevailing northeast dip north of the MAZ (EL-Naby et al. 2009). It reveals also alternative horsts and grabens delineated by normal step-like faults (parallel to the Clysmic trend).

Seismic section GOS 87-206

The 2D interpreted section of the seismic line GOS 87–206 is represented in Fig. 17. This line passes through the northern part of the study area (at southernmost part of the BDP, Fig. 15). A group of simple normal step faults in the NE (dipping towards the SW) and another set of faults in the SW (dipping towards NE) were observed along the section. These faults are parallel to the Clysmic trend and delineate a graben with a NW–SE running axis.

Seismic section AP 39

Figure 18 exhibits the 2D interpreted section of the seismic line AP 39. It cuts the southern part of BDP passing through

the northern part of MAZ (parallel to the Clysmic trend) and running parallel to line MP 89 (Fig. 15). This section reveals the northern boundary of the MAZ. North of this accommodation zone, a graben is bounded by two sets of oppositely dipping normal step-like cross faults (EL-Naby et al. 2009).

Seismic section MP 89

The seismic line MP 89 is running through the southern part of BDP and the uppermost northern boundary of MAZ (Fig. 15). The 2D interpreted seismic section of this line in shown in Fig. 19. A group of simple normal step faults in the NW (dipping towards the SE) and another set of faults in the SE (dipping towards NW) were observed in the northernmost part of this accommodation zone. These two sets of NE–SW-oriented faults are referred to as cross faults (Patton et al. 1994). These faults are perpendicular to the Clysmic trend and delineate a graben with a NE–SW running axis. North of this zone, a horst is located at the central part of the seismic section and is bounded between two sets of oppositely dipping normal step-like cross faults.

Fig. 22 Interpreted seismic section GOS 87–207, East Morgan oil field, Gulf of Suez
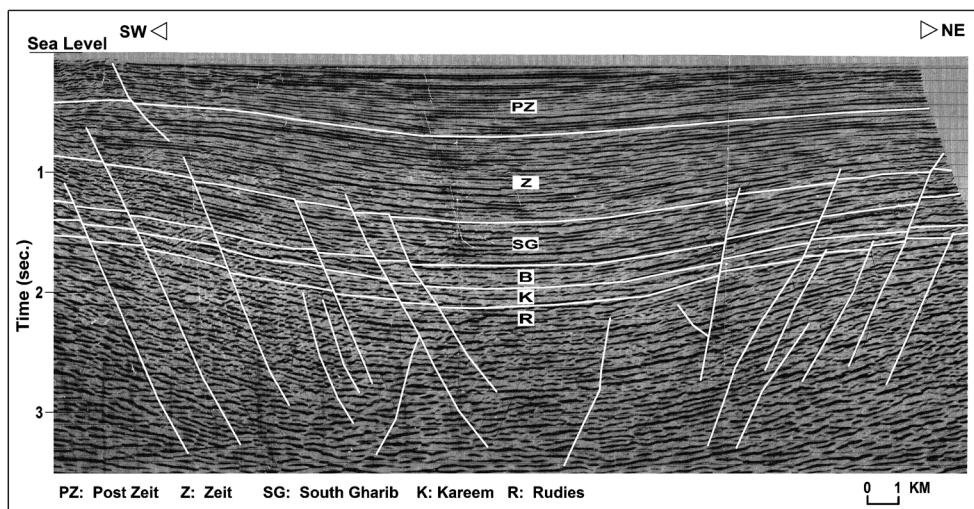
Table 3 Correlation between the major depositional sequences (S1 and S2) of the studied Miocene succession in the southwestern part of the Gulf of Suez with the genetic stratigraphic sequences (GSS) of the Arabian Plate tectono-stratigraphic mega-sequence AP11, based on stage correlation

Southwestern part of the Gulf of Suez			Arabian Plate				
Age	Sequences	Formations	MFS/TMS	Age (Ma)	Ages/Stages	Epochs/Series	Periods/System
Pliocene - Recent		Post Zeit		2	Pleistocene-Holocene		
					Gelasian		
					Piacenzian	L	Pliocene
				4	Zanclean	E	
Late Miocene	DSB2	Zeit		6	Messinian	Late	
	S2	South Gharib		8	Tortonian		
				10			
Middle Miocene		Belayim	Ng40	12	Serravallian	Middle	Neogene
			GSS40	14	Langhian		
	DSB1	Kareem	Ng30	16			Miocene
Early Miocene	S1	Rudeis	GSS30		Burdigalian	Early	
			Ng20	18			
			GSS20	20			
				22	Aquitanian		
			Ng10				

AP11 (spanning Age column region)

Modified after Sharland et al. 2001; Haq and Al-Qahtani 2005

DSB depositional sequence boundary, *MFS* maximum flooding surface, *TMS* tectono-stratigraphic mega-sequence

Seismic section GOS 86-24

Figure 20 represents the 2D interpreted seismic section GOS 86–24 that runs nearly parallel to line MP 89 and passes through the northern part of the MAZ (Fig. 15). This section illustrates that the Miocene horizons within this MAZ zone are influenced by syn-depositional normal step-like cross faults in the form of a wide graben (Younes and McClay 2002).

Seismic section GOS 87-301

The seismic line GOS 87–301 is passing through the northernmost part of the MAZ (Fig. 21). It runs parallel to lines GC 32 and GOS 87–206 in the southern part of BDP and GOS 87–207 in the northern part of the MAZ. This section reflects a wide graben with a NW–SE running axis. Two groups of simple normal step faults dipping towards NE in the southwestern part of the section and towards SW in the northeastern part are bounding this graben.

Seismic section GOS 87-207

Figure 22 clarifies the 2D interpreted seismic section GOS 87–207 passing through the northern part of the MAZ and running parallel to line GOS 87–301. This section outlines also a similar graben, like that in line GOS 87–301, with a NW–SE running axis. This wide graben is bounded by two sets of oppositely dipping normal step-like cross faults.

Sequence definition and seismic facies descriptions

The studied Miocene succession in the southwestern part of the Gulf of Suez is subdivided into two major third-order depositional sequences (S1 and S2). Table 3 shows the correlation of these major depositional sequences, which are separated by the two major depositional sequence boundaries (DSB1 and DSB2), with the genetic stratigraphic sequences (GSS20, GSS30 and GSS40). These genetic sequences represent the major tectono-stratigraphic mega-sequence (AP11) of the Arabian Plate according to Sharland et al. (2001) and Haq and Al-Qahtani (2005). These genetic stratigraphic sequences are separated by the maximum flooding surfaces MFS N20 and MFS Ng30, respectively (Figs. 23 and 24).

Sequence 1

The first sequence (S1) is represented by the Lower–Middle Miocene rocks, including the Rudeis and Kareem Formations. The top of this sequence is bounded by the depositional sequence boundary (DSB1), while the base of this sequence cannot be indicated in the seismic sections due to bad traces.

The seismic facies of this sequence are characterized by low to moderate amplitude and discontinuous horizons (Fig. 23). The reflection geometry at the cycle boundaries is considered as erosional truncation, toplaps and even concordant along the upper boundary of the cycle. The external form of these sediments is considered as sheet-like and wedge-shaped units.

The principal internal configurations appear to be parallel to chaotic, and the configuration modifier is generally regular. Generally, the Rudeis Formation is subdivided into two units: Lower Rudeis and Upper Rudeis that are both separated by the 'mid-Rudeis' or 'mid-Clysmic' event (Bosworth and McClay 2001). The facies of the Lower Rudeis Formation is composed mainly of calcareous shale and argillaceous limestone with a few shale and sandstone interbeds, which was deposited in an open-marine environment (middle to outer neritic; Bosworth 1995; Bosworth and McClay 2001; Lashin and Abd El-Aal 2004).

The Upper Rudeis Formation consists mainly of calcareous shale, argillaceous limestone and sandstone, which were deposited by episodic of depositional events produced under aqueous winnowing flow initiated by turbidity and storm-induced currents. The sliding and detachment of big blocks near to the rift margin has contributed the sediments accumulation, which reflect a rapid rate of accumulation in the basin floor and result in lenticular bodies formation (Lashin and Abd El-Aal 2004). The depositional environment of this part ranges from shallow to open marine that is mainly affected by the structural framework developed during the Early–Middle Miocene time. On the other hand, the depositional environment of the Kareem Formation ranges from local restricted lagoons to upper bathyal settings (see Abd El-Naby 2010). Furthermore, this third-order sequence is mostly equivalent to the upper part of GSS20 and GSS30 (Figs. 23 and 24). The GSS20 is interpreted as a 'third-order' succession with the overlying MFS Ng20 driven by subsidence enhanced by eustacy (Sharland et al. 2001). This subsidence may be equivalent to the rapid subsidence of 'mid-Clysmic' event during the deposition of the upper Rudeis Formation. The MFS Ng20 is dated as Burdigalian according to Motiei (1993). In the study area, this surface may coincide with the limestones of the upper part of Upper Rudeis Formation (see also Sharland et al. 2001; Figs. 23 and 24).

The GSS30 is interpreted as a 'second-order' succession with the overlying MFS Ng30 driven by subsidence enhanced by eustacy (Sharland et al. 2001). This subsidence may also coincide with the subsidence of 'mid-Clysmic' event, which continued during the deposition of the Kareem Formation. The MFS Ng30 may be equivalent to the MFS2 of the second sequence of the Kareem Formation (see Abd El-Naby 2010).

Sequence 2

The second sequence (S2) is represented by the Middle–Upper Miocene rocks, including the Belayim, South Gharib
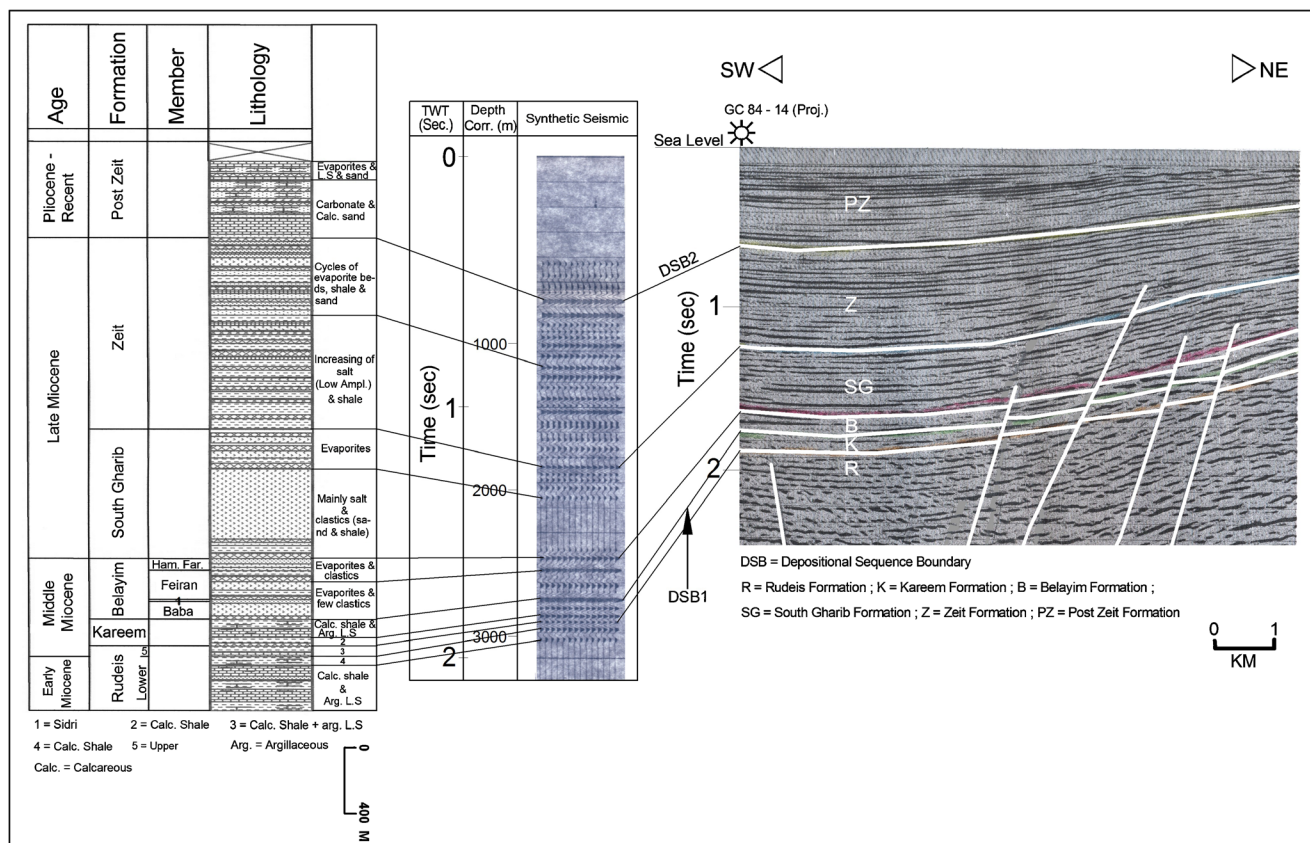
Fig. 23 Miocene lithological succession (*left*) correlated with a synthetic seismogram of GC 84–14 well (*middle*) and a seismic profile (eastern part of line GOS 87–301)

and Zeit Formations (Figs. 23 and 24). This sequence is bounded by the depositional sequence boundaries DSB1 and DSB2 (Figs. 23 and 24). The seismic facies of this sequence is characterized by high amplitude and continuous horizons (Fig. 23). The reflection geometry at the sequence boundaries is considered concordant and exhibits even toplaps along the upper boundary of the cycle. Downlaps and concordant reflection geometries are observed along the lower boundary. The external form of these sediments is considered as sheet-like and wedge-shaped units. The principal internal configurations appear to be parallel to divergent, and the configuration modifier is generally regular.

This sequence reflects abrupt changes of facies 'mainly to evaporites' during the deposition of Belayim Formation accompanied by a marked decrease in subsidence rate. The development of these evaporites appears to have occurred through the restriction of the Gulf from the Mediterranean by a structural high in the northern Gulf (Patton et al. 1994). Furthermore, the dominant salt deposition of South Gharib Formation is likely controlled by the restriction between the Gulf and the Mediterranean in the earliest Tortonian coupled with a significant fall in global eustatic sea level

(Haq et al. 1987). This process is associated with mild extension and subsidence of the southern Gulf (Bosworth et al. 1998).

This extension and subsidence continued during the deposition of Zeit Formation, which has been limited in age by Richardson and Arthur (1988) to the Messinian (5 Ma). Moreover, the depositional environment of this sequence is considered to be lagoonal to shallow marine environment. On the other hand, the lower part of this third-order sequence is mostly equivalent to the GSS40 (Figs. 23 and 24). The GSS40 is interpreted as a 'third-order' succession with the overlying MFS Ng40 driven by subsidence (Sharland et al. 2001). According to Sharland et al. (2001), this MFS Ng40 is dated as Late Serravallian. In the study area, the MFS Ng40 may span with the shales of the upper part of the Late Serravallian Belayim Formation (Figs. 23 and 24).

The Post-Miocene rocks are characterized by moderate to high amplitude, continuous, baselaps and concordant along lower boundary, sheet-like and wedge-shaped external forms, parallel to divergent internal reflection configuration and of regular nature. These features exhibit cycles of carbonates, evaporites and clastic deposits (sand and shale) of lagoonal environment.
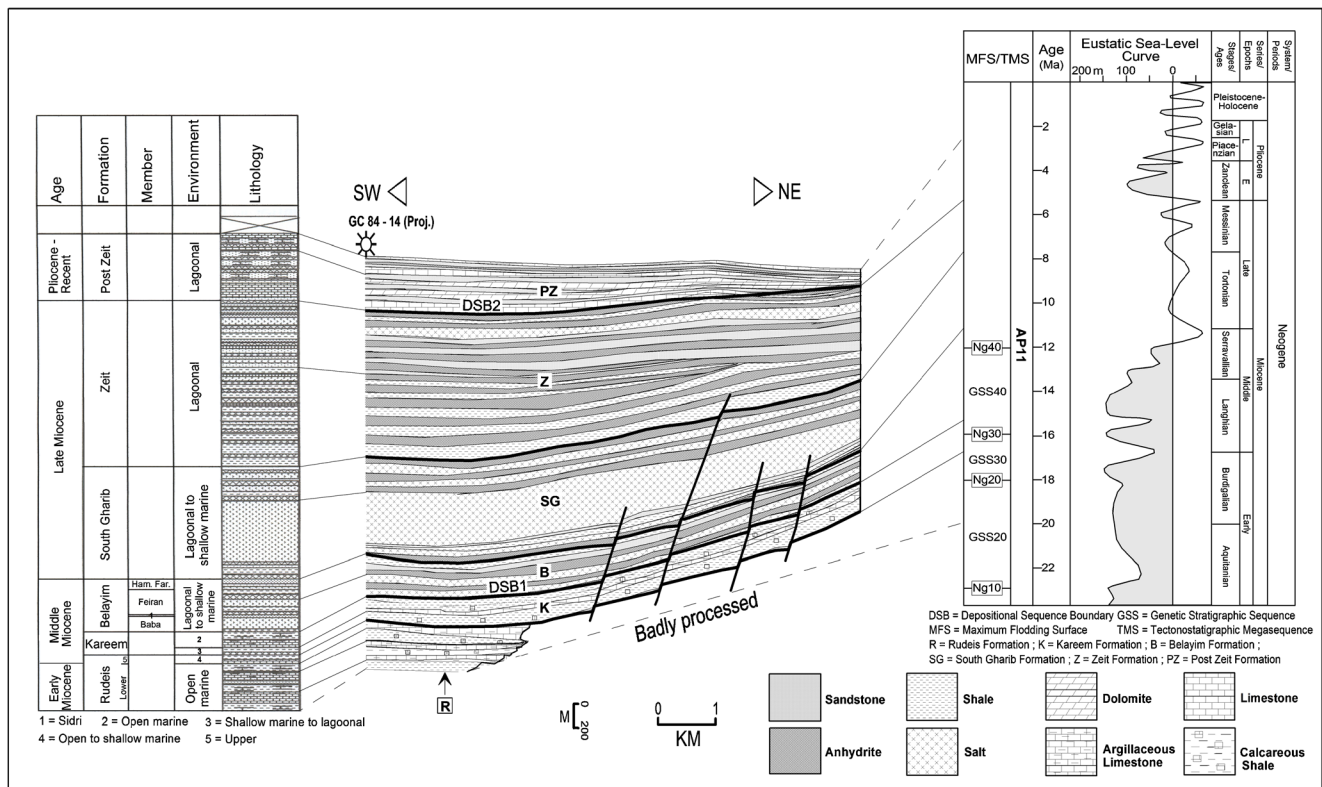
Fig. 24 Correlation between the Miocene lithological succession (*left*), the major interpreted depositional sequence boundaries of seismic depth profile GOS 87–30 (*middle*) and the Arabic Platform cycle chart 'modified after Sharland et al. 2001; Haq and Al-Qahtani 2005' (*right*)

Hydrocarbon potentiality and entrapment style

From the interpretation of the petrophysical data and analysis of seismic data, the western middle part of the PDB zone is the best area for hydrocarbon potentiality. This area is occupied by SG310-4, J37-43A, SG310-6A and SG310-7A wells and show good petrophysical parameters, in terms of thick sand reservoir (120 m), average values of good effective porosity (8 %), low shale volume (20 %), low water saturation (60 %) and good hydrocarbon content (40 %).

The seismic structural and sequence analyses show that the hydrocarbon-bearing reservoirs are belonging to the third-order depositional sequence S1 that represents the Lower–Middle Miocene rocks (Asl and Hawara Formations) and mainly dissected by a number of successive step-like normal faults. The facies of the reservoirs are mainly clastics (sandstone), characterized by low to moderate amplitude.

The entrapment of hydrocarbons seems to be due to a combined effect of the stratigraphic and structural elements. It appears clear that both of the step-like structural fault system and the lateral variation of facies are the key parameters that control the accumulation of hydrocarbon in this area and in East Morgan field as a whole. For development purposes, this area is the best for drilling new further wells.

Conclusions

The main concluded points from this study can be summarized as the follows:

– East Morgan oil field is one of the promising oil fields that are located in the southern part of the Gulf of Suez. The most important hydrocarbon-bearing reservoirs are encountered in the Early–Middle Miocene deposits (Asl and Hawara Formations).

– The petrophysical analysis revealed the presence of good oil saturation in the sand sections of Asl Formation in the BDP.

– The average petrophysical parameters of Asl reservoir throughout the study area range between 4 % and 10 % for effective porosity, 18 % and 89 % for shale volume and 2 % and 48 % for hydrocarbon saturation.

– Fair to good oil saturations are assigned for Hawara Formation (1–8 %, 20–98 % and 2–32 % for effective porosity, shale volume and hydrocarbon saturation, respectively).

– Little hydrocarbon saturation is represented by both formations to the south of the study area in the MAZ.

– The seismic data analysis shows that the whole succession in the study area (including the reservoir rocks) is

dissected by a group of simple NW–SE step-like normal faults, parallel to the Clysmic trend. Some graben- and horst-shaped structures are found and usually bounded by two sets of oppositely dipping normal step-like cross faults.

- The seismic sequence stratigraphy study clarified that the main hydrocarbon-bearing reservoirs in the study area (Asl and Hawara Formations that are equivalent to Rudeis Formation) belong to the S1 sequence of the major two third-order depositional sequences in the Gulf of Suez.

- The seismic facies of this sequence (S1) are characterized by low to moderate amplitude, discontinuous horizons and bounded by the depositional sequence boundary (DSB1) at the top. The reflection geometry at the cycle boundaries is considered as an erosional truncation, toplaps and even concordant along the upper boundary of the cycle.

- The depositional environment is shallow to open marine environments, mainly affected by the structure framework developed during the Early–Middle Miocene time.

- The second sequence (S2) is represented by the Middle–Upper Miocene rocks, including the Belayim, South Gharib and Zeit Formations. The sequence is characterized by seismic facies of high-amplitude continuous horizons, concordant reflection geometry (toplaps along the upper boundary and downlaps along lower boundary) and sheet-like and wedge-shaped internal configurations of these units.

- The environment of deposition of this sequence reflects abrupt facies changes accompanied by a marked decrease in subsidence rate. It is considered to be lagoonal to shallow marine.

- The integrated interpretation of the petrophysical data (vertical data logs and lateral distribution maps) and the seismic data analysis revealed that the western middle part of the PDB zone is the best in terms of the hydrocarbon potentiality that it attains and the structural elements that controls the accumulation of the hydrocarbons. For development purposes, this area is very good for drilling new wells.

References

Abd El-Gawad M (1970) The Gulf of Suez: a brief review of stratigraphy and structure. Phil Trans Roy Soc London A267:41–48

Abd El-Naby A, Abd El-Aal M, Kuss J, Boukharay M, Lashin A (2009) Structural and basin evolution in Miocene time, Southwestern Gulf of Suez, Egypt. Neues Jahrbuch für Geologie und Paläontologie-Abhandlungen, Germany 251(3):331–353

Abd El-Naby A, Abd El-Aal M, Kuss J, Boukharay M (2010) Stratigraphy interpretation of structurally controlled deposition: Middle Miocene Kareem Formation, southwestern Gulf of Suez, Egypt. GeoArabia 15(3):129–150

Al-Arifi N, Lashin A, Al-Humidan S (2012) Migration of local earthquakes in the Gulf of Aqaba, Saudi Arabia. Earth Sci Res SJ 16(1):35–40

Bobbit JE, Gallagher JD (1978) The petroleum geology of the Gulf of Suez. Tenth Annual Offshore Technical Conference, Houston, Texas, pp 375–380

Robson DA (1971) The structure of the Gulf of Suez (Clysmic) rift with special reference to the eastern side. J Geol Soc Lond 127:247–277

Bosworth W (1985) Geometry of propagating continental rifts. Nature 316:625–627

Bosworth W (1995) A high-strain rift model for the southern Gulf of Suez (Egypt). In: Lambiase JJ (ed) Hydrocarbon habitat in rift basins. Geological Society of London Special Publications 80:75–112

Bosworth W, McClay K (2001) Structural and stratigraphic evolution of the Gulf of Suez rift, Egypt: a synthesis. In: Ziegler PA, Cavazza W, Robertson AHF, Crasquin-Soleau S (eds) Peri-Tethys Memoir 6: Peri-Tethyan rift/wrench basins and passive margins. Museum National d'Histoire naturelle de Paris Memoirs 186:567–606

Bosworth W, Crevello P, Winn RD Jr, Steinmetz J (1998) Structure, sedimentation, and basin dynamics during rifting of the Gulf of Suez and the northwestern Red Sea. In: Purser BH, Bosence DWJ (eds) Sedimentation and tectonics of rift basins: Red Sea-Gulf of Aden. Chapman and Hall, London, pp 77–96

Coffield DQ, Schamel S (1989) Surface expression of an accommodation zone within the Gulf of Suez rift, Egypt. Geology 17:76–79

Emery D, Myers K (1996) Sequence stratigraphy. Blackwell Science Ltd., Oxford, 297 p

Garfunkel RL, Bartov Y (1977) The tectonic of the Suez rift. Bull Geol Surv Isr 71:1–44

Gawthorpe RL, Hurst JM (1993) Transfer zones in extensional basins: their structural style and influence in drainage development and stratigraphy. J Geol Soc 150:1137–1152

Haq BU, Al-Qahtani AM (2005) Phanerozoic cycles of sea-level change on the Arabian Platform. GeoArabia 10(2):127–160

Haq BU, Hardenbol J, Vail PR (1987) Chronology of fluctuating sea level since the Triassic. Science 235:1156–1167

Khalil BA (1984) Geological and sedimentological studies of Oligo-Miocene section in Abu Zenima area and October Field. MSc thesis. Geology Department, Ain Shams University, Cairo

Hagras M (1986) Some geological observation in the Gulf of Suez area. Egypt, Eighth EGPC Exploration Conference, Cairo

Harper ML (1966) Block faulting and sedimentation in the Gulf of Suez. Unpublished internal company report, 36 p

Hassouba A, Sarrawi M, Sakr S (1994) Early syn-rift sedimentation in October field area: a stratigraphic model for hydrocarbon accumulation. Twelfth Petroleum Exploration and Production Conference, Cairo, pp 341–350, Part I of II

Hataba H, Hosny W, Gaafar I (1990) Application of graphic technique on the Miocene stratigraphy in October field area, Gulf of Suez. Tenth Petroleum Exploration and Production Conference, Cairo, pp 320–344, Part I

Lashin A, Abd El-Aal M (2004) Seismic data analysis to detect the depositional process environments and structural framework of the east central part of Gharib Province, Gulf of Suez-Egypt. Annals of the Egyptian Geological Survey 27:523–550

Lashin A, Al-Arifi N, Abu Ashour N (2011) Evaluation of the ASL and Hawara Formations using seismic- and log-derived properties, October oil field, Gulf of Suez, Egypt. Arab J Geosci 3–4:365–383

Lashin A, Mogren S (2012) Total organic carbon enrichment and source rock evaluation of the Lower Miocene rocks based on well logs: October oil field, Gulf of Suez-Egypt. Int J Geosci 3:683–695

Lashin A, Serag El Din S (2012) Reservoir parameters determination using artificial neural networks: Ras Fanar field, Gulf of Suez, Egypt. Arab J Geosci. doi:10.1007/s12517-012-0541-6

Lyberis N (1988) Tectonic evolution of the Gulf of Suez and the Gulf of Aqaba. Tectonophysics 153:209–220

Mesheref WM, Rafel EM, Abdel Baki SH (1976) Structural interpretation of the Gulf of Suez and its oil potentialities. Third EGPC Exploration Seminar, Cairo

Meshref W, Abu El-Karamat M, El-Gindi M (1988) Exploration concept for oil in the Gulf of Suez. Ninth EGPC Exploration Conference, Cairo

Motiei H (1993) Stratigraphy of Zagros. Treatise on the Geology of Iran No. 1, Ministry of Mines and Metals. Geological Survey of Iran, Tehran

Moustafa AM (1976) Block faulting of the Gulf of Suez. Fifth Exploration Seminar, unpublished report. Egyptian General Petroleum Corporation, Egypt, pp 1–19

Patton TL, Moustafa AR, Nelson RA, Abdine SA (1994) Tectonic evolution and structural setting of the Suez Rift. In: Landon SM (ed) Interior rift basins. AAPG Memoirs 59:7–55

Posamentier HW, Weimer P (1993) Siliciclastic sequence stratigraphy and petroleum geology—where to from here? AAPG Bull 77:731–742

Rashed A (1990) The main fault trends in the Gulf of Suez and their role in oil entrapment. Tenth Petroleum exploration and production Conference, Cairo, pp 43–178, Part I

Richardson M, Arthur MA (1988) The Gulf of Suez-northern Red Sea Neogene rift: a quantitative basin analysis. Mar Pet Geol 5:247–270

Schlumberger (1984) Well evaluation conference—Egypt. France, pp. 1–60

Schlumberger (1995) Well evaluation conference—Egypt. Houston, Texas, pp. 1–87

Shahin AN (1992) Oil window in the Gulf of Suez and the Northern Red Sea area. First International Symposium on Sedimentation and Rifting the Red Sea and Gulf of Aden, Egypt

Shahin AN, Shehab MM (1984) Petroleum generation, migration and accumulation in the Gulf of Suez offshore, Sinai, vol 1. Sixth EGPC Exploration Seminar, Egypt, pp 126–152

Shahin NA, Hassouba A, Sharaf LM (1994) Assessment of petroleum potential in the Northern Gulf of Suez. Twelfth Petroleum Exploration and Production Conference, Cairo, November, Part I of II, pp 152–174

Sharland PR, Archer R, Casey DM, Davies RB, Hall SH, Heward AP, Horbury AD, Simmons MD (2001) Arabian plate sequence stratigraphy. GeoArabia 2:371

Soliman OM (1988) Petroleum habitat in the vicinity of October oil Field. Suez Canal University, Suez, Gulf of Suez. MSc thesis

Vail PR, Mitchum RM Jr, Thompson S (1977a) Seismic stratigraphy and global changes of sea-level. Part 3: relative changes of sea-level from costal onlap. In: Pyton CE (eds) Seismic stratigraphy—applications to hydrocarbon exploration. AAPG Spec Mem 26:63–82

Vail PR, Mitchum RM Jr, Thompson S (1977b) Seismic stratigraphy and global changes of sea-level. Part 4: global cycles of relative changes in sea-level. In: Pyton CE (ed) Seismic stratigraphy—applications to hydrocarbon exploration. AAPG Spec Mem 26:83–97

Vail PR (1987) Seismic stratigraphy interpretation procedure. In: Bally AW (ed) Atlas of seismic stratigraphy, AAPG Studies in Geology 27(1):1–10

Van Wagoner JC, Posamentier HW, Mitchum RM, Vail PR, Sarg JF, Loutit TS, Hardenbol J (1988) An overview of the fundamentals of sequence stratigraphy and key definitions. In: Wilgus CK, Hastings BC, Kendall CG, Posamentier HW, Ross CA, Van Wagoner JC (eds) Sea-level changes: an integrated approach. Soc Econ Plaeo Miner Spec Pub 42:39–45

Van Wagoner JC, Mitchum RM, Campion KM, Rahmanian VD (1990) Siliciclastic sequence stratigraphy in well logs, cores and outcrops; concepts for high resolution correlation of time and facies. AAPG Methods in Exploration 7:55

Younes AI, McClay K (2002) Development of accommodation zones in the Gulf of Suez-Red Sea rift, Egypt. AAPG 86:1003–1026